JOURNAL OF GEOPHYSICAL RESEARCH, VOL. 114, G01018, doi:10.1029/2007JG000675, 2009

Influence of clouds and diffuse radiation on ecosystem-atmosphere CO_2 and $CO^{18}O$ exchanges

C. J. Still,[1,2] W. J. Riley,[3] S. C. Biraud,[3] D. C. Noone,[4] N. H. Buenning,[4] J. T. Randerson,[5] M. S. Torn,[3] J. Welker,[6] J. W. C. White,[7] R. Vachon,[7] G. D. Farquhar,[8] and J. A. Berry[9]

Received 20 December 2007; revised 11 November 2008; accepted 2 December 2008; published 4 March 2009.

[1] This study evaluates the potential impact of clouds on ecosystem CO_2 and CO_2 isotope fluxes ("isofluxes") in two contrasting ecosystems (a broadleaf deciduous forest and a C_4 grassland) in a region for which cloud cover, meteorological, and isotope data are available for driving the isotope-enabled land surface model (ISOLSM). Our model results indicate a large impact of clouds on ecosystem CO_2 fluxes and isofluxes. Despite lower irradiance on partly cloudy and cloudy days, predicted forest canopy photosynthesis was substantially higher than on clear, sunny days, and the highest carbon uptake was achieved on the cloudiest day. This effect was driven by a large increase in light-limited shade leaf photosynthesis following an increase in the diffuse fraction of irradiance. Photosynthetic isofluxes, by contrast, were largest on partly cloudy days, as leaf water isotopic composition was only slightly depleted and photosynthesis was enhanced, as compared to adjacent clear-sky days. On the cloudiest day, the forest exhibited intermediate isofluxes: although photosynthesis was highest on this day, leaf-to-atmosphere isofluxes were reduced from a feedback of transpiration on canopy relative humidity and leaf water. Photosynthesis and isofluxes were both reduced in the C_4 grass canopy with increasing cloud cover and diffuse fraction as a result of near-constant light limitation of photosynthesis. These results suggest that some of the unexplained variation in global mean $\delta^{18}O$ of CO_2 may be driven by large-scale changes in clouds and aerosols and their impacts on diffuse radiation, photosynthesis, and relative humidity.

Citation: Still, C. J., et al. (2009), Influence of clouds and diffuse radiation on ecosystem-atmosphere CO_2 and $CO^{18}O$ exchanges, *J. Geophys. Res.*, *114*, G01018, doi:10.1029/2007JG000675.

1. Introduction

[2] While spatial and temporal variations in atmospheric CO_2 and its $^{13}C/^{12}C$ composition have received considerable attention from the carbon cycle community [e.g., *Ciais et al.*, 1995; *Fung et al.*, 1997; *Rayner et al.*, 1999, 2008; *Randerson et al.*, 2002a, 2002b; *Scholze et al.*, 2003], much less is known about the $^{18}O/^{16}O$ composition of atmospheric CO_2 ($\delta^{18}O_a$; symbols defined in Table 1). Although global simulations of $\delta^{18}O_a$ and its controlling processes have made good progress [*Farquhar et al.*, 1993; *Ciais et al.*, 1997a, 1997b; *Peylin et al.*, 1999; *Cuntz et al.*, 2003a, 2003b; N. Buenning et al., Modeling the response of the terrestrial biosphere and $\delta^{18}O$ of atmospheric CO_2 to flux, humidity, and isotope hydrology changes, manuscript in preparation, 2009], fundamental spatial and temporal variations of $\delta^{18}O_a$ are poorly captured by state-of-the-art global model simulations. One example of unexplained behavior is the phase shift between seasonal cycles of CO_2 and $\delta^{18}O_a$ observed at high northern latitudes, though a recent study showed how this shift is sensitive to boreal forest plant functional type composition and the $\delta^{18}O$ of plant source water [*Welp et al.*, 2006]. A second, outstanding example of unexplained variation is the large, multiyear variation in mean $\delta^{18}O_a$ observed at many stations. The pronounced downward excursion in global mean $\delta^{18}O_a$ observed during the early and mid-1990s averaged ~ -0.1‰ a^{-1} for extratropical, marine boundary layer stations, implying isotope fluxes, or "isofluxes," on the order of tens of Pmol CO_2‰ a^{-1}.

[3] Because $\delta^{18}O_a$ is strongly influenced by exchanges of $CO^{18}O$ between the atmosphere and terrestrial ecosystems

[1]Department of Geography, University of California, Santa Barbara, California, USA.
[2]Institute for Computational Earth System Science, University of California, Santa Barbara, California, USA.
[3]Earth Sciences Division, Lawrence Berkeley National Laboratory, Berkeley, California, USA.
[4]Department of Atmospheric and Oceanic Sciences and Cooperative Institute for Research in Environmental Science, University of Colorado, Boulder, Colorado, USA.
[5]Earth System Science Department, University of California, Irvine, California, USA.
[6]Environment and Natural Resources Institute, University of Alaska, Anchorage, Alaska, USA.
[7]INSTAAR and Cooperative Institute for Research in Environmental Science, University of Colorado, Boulder, Colorado, USA.
[8]Research School of Biological Sciences, Australian National University, Canberra, ACT, Australia.
[9]Department of Global Ecology, Carnegie Institution of Washington, Stanford, California, USA.

0148-0227/09/2007JG000675$09.00

Table 1. Nomenclature Used in the Paper[a]

Variable	Description
$\delta^{18}O_a$	Background atmosphere δ^{18}O-CO_2 (VPDB-CO_2)
R_D/R_S	Diffuse fraction, the ratio of diffuse irradiance to total (global) irradiance or of diffuse PAR to total PAR
PAR	Photosynthetically Active Radiation (400–700 nm).
LAI	Leaf area index (m^2/m^2)
$^{18}\Delta$	Discrimination against $CO^{18}O$ during photosynthesis
ε_d	Kinetic fractionation during molecular diffusion of $CO^{18}O$
$\delta^{18}O_c$	δ^{18}O value of CO_2 in equilibrium with H_2O in leaves
Ca, *Ci*, *Cc*	CO_2 concentrations in the atmosphere, stomatal pore, and in chloroplasts
F_{al}	Gross CO_2 flux from atmosphere to leaf
F_{la}	Gross CO_2 flux from leaf to atmosphere
A_{net}	Net leaf photosynthesis including leaf respiration (F_{al}-F_{la})
$^{18}F_{al}$	Atmosphere-to-leaf isoflux (δ^{18}O in CO_2)
$^{18}F_{la}$	Leaf-to-atmosphere isoflux (δ^{18}O in CO_2)
$A_{net}{}^{18}\Delta$	Net photosynthetic isoflux
$\delta^{18}O_{lw}$	δ^{18}O value of leaf water (VSMOW)
$\delta^{18}O_{xy}$	δ^{18}O composition of source water in xylem (VSMOW)
$\delta^{18}O_{sw}$	δ^{18}O composition of soil water (VSMOW)
$\delta^{18}O_{cv}$	δ^{18}O composition of in-canopy water vapor (VSMOW)
$\delta^{18}O_v$	δ^{18}O composition of background, above-canopy water vapor (VSMOW)

[a]Here $\delta = \left(\frac{R_{sam}}{R_{std}} - 1\right)$ and R_{sam} and R_{std} are the ratios of $^{18}O/^{16}O$ in a sample or standard, respectively. The δ^{18}O-CO_2 values are reported relative to the

during photosynthesis and respiration [*Francey and Tans*, 1987; *Friedli et al.*, 1987; *Farquhar et al.*, 1993; *Ciais et al.*, 1997a, 1997b; *Cuntz et al.*, 2003a, 2003b], several studies have related the downward excursion of $\delta^{18}O_a$ to terrestrial carbon cycle anomalies [*Gillon and Yakir*, 2001; *Stern et al.*, 2001; *Ishizawa et al.*, 2002; *Flanagan*, 2005]. However, water cycle anomalies can also affect $\delta^{18}O_a$, as the δ^{18}O of ecosystem-to-atmosphere CO_2 fluxes is determined by the δ^{18}O of leaf and soil water pools which interact with CO_2 during photosynthesis and respiration [*Yakir and Sternberg*, 2000]. Leaf and soil water δ^{18}O are in turn determined by the δ^{18}O of precipitation [*Welker*, 2000; *Vachon et al.*, 2007] and water vapor and subsequent isotopic fractionations during evaporation and diffusion [*Craig and Gordon*, 1965; *Allison et al.*, 1983]. Although either carbon or water cycle anomalies may drive $\delta^{18}O_a$, unexplained multiyear variations in $\delta^{18}O_a$ such as occurred in the 1990s likely result from linked perturbations to both cycles.

[4] Recent research has documented large variability in tropical cloud cover [e.g., *Wielicki et al.*, 2002] on interannual timescales that span part of the $\delta^{18}O_a$ record. For example, satellite measurements of earth's shortwave and longwave radiation budgets over the 1990s suggest decreases in tropical mean cloudiness [*Wielicki et al.*, 2002], in agreement with decreases in the monthly mean global cloud fraction over the 1990s (http://isccp.giss.nasa.gov/climanal1.html). Tropical cloud cover variability may be particularly relevant for understanding global $\delta^{18}O_a$ variations, as tropical terrestrial ecosystem CO_2 fluxes comprise a large fraction of global productivity. Other satellite-based analyses document increasing spring and summer cloud cover in the Arctic region [*Wang and Key*, 2003]. In addition, evidence from ground-based radiometers suggests secular changes in surface global irradiance, with a total reduction of ~4–6% from about 1960 to 1990 ("global dimming") [*Stanhill and Cohen*, 2001; *Liepert*, 2002; *Liepert et al.*, 2004] followed by a reversal from roughly 1990 onward that has been termed "global brightening" [*Wild et al.*, 2005, 2007; *Pinker et al.*, 2005; *Roderick*, 2006].

[5] Here we examine the hypothesis that these large-scale changes in cloud cover and irradiance account for part of the unexplained variation observed in $\delta^{18}O_a$, as clouds influence several environmental factors important in controlling biosphere-atmosphere CO_2 isofluxes. Clouds reduce total shortwave (global) irradiance (R_S) while also increasing diffuse irradiance (R_D) and the diffuse fraction (R_D/R_S, the ratio of diffuse irradiance to total or global irradiance [*Roderick*, 1999]). Numerous empirical and theoretical studies have noted the impact of changes in diffuse photosynthetically active radiation (PAR) on canopy carbon uptake via increases in photosynthesis of light-limited shade leaves and other associated changes in the environment [e.g., *Price and Black*, 1990; *Hollinger et al.*, 1994, 1998; *Gower et al.*, 1999; *Choudhury*, 2001; *Roderick et al.*, 2001; *Freedman et al.*, 2001; *Gu et al.*, 1999, 2002, 2003; *Rocha et al.*, 2004; *Min*, 2005; *Urban et al.*, 2007; *Oliveira et al.*, 2007; *Knohl and Baldocchi*, 2008]. In addition to increasing R_D/R_S and the contribution of shade leaves to canopy photosynthesis, clouds decrease radiant heating of upper canopy sun leaves, potentially increasing net photosynthetic rates [*Roderick et al.*, 2001; *Gu et al.*, 2002, 2003]. Increased cloudiness is often also associated with higher surface relative humidity via decreases in air and leaf temperature and increases in specific humidity [*Freedman et al.*, 2001].

[6] Relative humidity will influence both photosynthetic CO_2 fluxes and the δ^{18}O of leaf water via impacts on stomatal conductance, and thus can have a disproportionate impact on ecosystem-atmosphere isofluxes. An increase in relative humidity generally increases stomatal conductance, which, coupled with increased shade leaf photosynthesis, should increase photosynthetic isofluxes. However, increased relative humidity will also decrease leaf water δ^{18}O because of a greater influx of depleted vapor, and this would decrease photosynthetic isofluxes.

[7] Thus, the *net* effect of changing cloud cover on biosphere-atmosphere CO_2 and CO_2 isofluxes exchanges is difficult to assess without high-frequency ecosystem $CO^{18}O$ flux measurements. However, these data are currently being

collected at only a few sites at present [*Griffis et al.*, 2008; *McDowell et al.*, 2008]. The focus of this study instead is to examine potential ecosystem isoflux responses using observed cloud cover, radiation, meteorological and water isotope data to drive an isotope-enabled ecosystem model (ISOLSM). We chose to focus on two contrasting ecosystems in the Southern Great Plains over a short time period for intensive investigation of the mechanisms underlying the modeled canopy isoflux response to changing cloud cover. For our analyses, we selected a 12-day period from 11 to 22 July 2004 (day of year (DOY) 193–204,) during which strong variations in daytime thick cloud cover occurred at our study site, from less than 10% on clear days to 100% on a cloudy day. In addition to cloud cover variations, we selected this period using the following criteria: constant LAI, only trace amounts of precipitation (since precipitation $\delta^{18}O$ is a primary driver of CO_2 isofluxes), and no large changes in air temperature and specific humidity due to the passage of differing air masses associated with storm fronts. By limiting variability from these factors, we decomposed the predicted isoflux response to cloud cover into its component processes.

2. Methods

2.1. Site Description

[8] To capture the relevant processes that determine the net impact of clouds on ecosystem $CO^{18}O$ isofluxes, we employed a comprehensive, isotope-enabled ecosystem model (ISOLSM) [*Riley et al.*, 2002, 2003; *Still et al.*, 2005] in the DOE Atmospheric Radiation Measurement (ARM) program's Climate Research Facility (ACRF) in the 140,000 km^2 Southern Great Plains (SGP) region of Oklahoma and Kansas [*Ackerman and Stokes*, 2003]. The SGP region is particularly amenable for such a study because of the great diversity of cloud property, aerosol, radiation, and meteorological measurements available, with the most intensive data collection at the Central Facility (CF) site near Lamont, OK (36° 36.30′N, 97° 29.10′W, 320 masl). Analysis of atmospheric data collected at the CF has shown large changes in irradiance driven by cloud cover from 1997 to 2004 [*Dong et al.*, 2006]. The SGP region also contains natural and agricultural ecosystems representing a variety of photosynthetic pathways and growth forms, including tallgrass prairies, broadleaf forests along riparian areas, and crops such as winter wheat, milo, and corn. Because we wanted to explore the impact of cloud cover variations on ecosystem-atmosphere isofluxes in two globally important but strongly contrasting natural vegetation types also represented within the SGP region, we chose broadleaf deciduous forests and C_4 grasslands for our model simulations.

2.2. Model Description

[9] ISOLSM is based on the NCAR Land Surface Model (LSM1.0) [*Bonan*, 1994; *Bonan et al.*, 1997], which was modified by *Riley et al.* [2002] to simulate the carbon and oxygen isotope composition of terrestrial ecosystem-atmosphere CO_2 and H_2O exchanges. The model simulates canopy radiation transfer using the two-stream approximation of *Dickinson* [1983] and *Sellers* [1985] to calculate direct and diffuse radiation fluxes in the visible and near-infrared wave bands. The canopy is divided into sunlit and shaded leaves using an extinction coefficient that accounts for scattering within the canopy [*Sellers*, 1985]. The model does not vary leaf nitrogen and photosynthetic capacity between sun and shade leaves, as is done in some models [e.g., *de Pury and Farquhar*, 1997; *Wang and Leuning*, 1998]. The version of ISOLSM applied here differs from that described by *Riley et al.* [2002] by several changes made to the plant photosynthesis submodels. First, low- and high-temperature inhibition factors on the maximum catalytic capacity of Rubisco (V_{max}) from *Sellers et al.* [1996] have been included. Second, we implemented the method of *Sellers et al.* [1996] to smooth transitions between the three limiting assimilation rates (i.e., Rubisco, light, and export limited). Finally, iterations to estimate C_c and C_i, the leaf chloroplast and internal CO_2 concentrations, are now performed using net photosynthesis (i.e., accounting for leaf respiration occurring inside the leaf), as opposed to gross photosynthesis, as done in the original version of LSM1. Of these changes, the last had the largest impact, resulting in values for V_{max} and C_i that are much closer to measured values. Accurate C_i and C_c are critical for simulating isotopic fractionations against $^{13}CO_2$ and $CO^{18}O$. ISOLSM models mesophyll (or internal) conductance in C_3 plants to be proportional to the maximum carboxylation capacity (V_{max} (in μmol m^{-2} s^{-1})) following *Evans and Loreto* [2000], but without the soil moisture dependence implemented by *Randerson et al.* [2002b]. During light-saturated photosynthesis in forest sun leaves, the average drawdown from C_i to C_c was ~4 Pa over the study period, similar to the drawdown measured by *Gillon and Yakir* [2000].

[10] We have tested ISOLSM's H_2O and CO_2 flux predictions against several sets of measurements: (1) in the dominant vegetation types using measurements [*Suyker and Verma*, 2001] performed in the SGP as part of the AmeriFlux program [*Riley et al.*, 2003]; (2) against 3 years of surface measurements made during the FIFE campaign [*Betts and Ball*, 1998; *Cooley et al.*, 2005]; (3) in a tallgrass prairie site in Kansas [*Lai et al.*, 2006a]; (4) in an old growth conifer forest in Oregon [*Aranibar et al.*, 2006]; and in more recent measurements in wheat, pasture, and soy (W. J. Riley et al., manuscript in preparation, 2009). We have also tested ISOLSM's isotopic predictions against available data in Great Plains grassland and cropland ecosystems (i.e., $\delta^{18}O$ in ecosystem water pools and fluxes, and $\delta^{18}O$ in ecosystem CO_2 fluxes [*Riley et al.*, 2003; *Still et al.*, 2005; *Lai et al.*, 2006a]). We have previously applied ISOLSM to examine (1) impacts of the atmospheric $\delta^{18}O$ value of H_2O and CO_2 on ecosystem discrimination against $CO^{18}O$ [*Riley et al.*, 2003]; (2) impact of carbonic anhydrase activity in soils and leaves [*Riley et al.*, 2002, 2003]; (3) impacts of gradients in the $\delta^{18}O$ value of near-surface soil water on the $\delta^{18}O$ value of the soil surface CO_2 flux [*Riley et al.*, 2003; *Riley*, 2005]; (4) impacts of land use change on regional surface CO_2 and energy fluxes and near-surface climate [*Cooley et al.*, 2005]; and (5) the use of ^{13}C measurements to improve model parameterizations [*Aranibar et al.*, 2006]. The isotope submodels in ISOLSM simulate the dominant processes impacting the $\delta^{18}O$ value of soil ($\delta^{18}O_{sw}$) and leaf H_2O ($\delta^{18}O_{lw}$) and CO_2 fluxes: advection of $H_2^{18}O$ in soil water and subsequent evaporation, leaf water isotopic enrichment, isotopic exchanges between H_2O and CO_2 in the soil and leaves, the transport of CO_2 and $CO^{18}O$ in the soil column, and the $\delta^{18}O$ of canopy water vapor ($\delta^{18}O_{cv}$). The xylem source water that supplies leaves,

$\delta^{18}O_{xy}$, is determined in ISOLSM by the vertical distribution of $\delta^{18}O_{sw}$, weighted by rooting density profiles for the various ecosystem types. $\delta^{18}O_{cv}$ is calculated at each time step as a function of vapor isotope exchanges with above-canopy air ($\delta^{18}O_v$), as well as isotope fluxes from canopy transpiration and soil and canopy evaporation when the canopy is wet [*Riley et al.*, 2002]. Further description of our leaf water $\delta^{18}O$ and photosynthetic isoflux calculations is given in section 3.

2.3. Cloud Cover, Radiation, Meteorology, and Water Isotope Forcing Data

[11] ISOLSM is forced with meteorological and water isotope data [*Riley et al.*, 2002, 2003], and it has recently been modified to ingest satellite measurements of vegetation characteristics such as the projected leaf area index (LAI). For the simulations reported here, radiation, cloud property, and aerosol data were acquired from instruments at the ARM Central Facility (CF) in Lamont, OK, which is the primary measurement facility within the ARM SGP region [*Ackerman and Stokes*, 2003]. The instrument array at the CF includes sensors to measure cloud presence and cloud radiative properties, which are necessary to explore the role of clouds in ecosystem-atmosphere $CO^{18}O$ exchanges. Radiation fluxes measured at the CF site include downwelling shortwave radiation (direct and diffuse) and downwelling longwave radiation. For our analysis, early morning and late afternoon values (solar angles less than 15°) were screened to minimize the impact of low solar angles on R_D/R_S.

[12] The ARM cloud data used are the daytime percent cover of clouds, as measured by the total sky imager (TSI), an instrument that measures the fractional sky coverage of thin and thick (opaque) clouds (i.e., the fraction of the hemispheric field of view that contains these cloud types) for daytime periods when the solar elevation exceeds 10 degrees. For this analysis, we focus on the percent cover of thick clouds, as these are both the dominant cloud types and have the largest impact on irradiance, R_D/R_S, temperature, and relative humidity. *Min* [2005] showed that diffuse radiation fluxes due to optically thick clouds have a greater impact on canopy photosynthetic efficiency than do fluxes from optically thin clouds. Because of temporal limitations on these data (i.e., only daytime cloud cover fractions are available from the TSI), we have restricted our analysis to daytime periods. Although nighttime clouds can affect the surface energy budget and carbon cycle through modulation of longwave energy fluxes [e.g., *Dai et al.*, 1999], the largest impacts of clouds on canopy isofluxes should occur during the day. Unfortunately, cloud-screened aerosol optical depth data from a Sun photometer [e.g., *Niyogi et al.*, 2004; *Oliveira et al.*, 2007] were not available for our study period to allow a separate assessment of aerosol impacts on isofluxes.

[13] The meteorological data used to force ISOLSM include air temperature, pressure, water vapor content, wind speed, and precipitation amount. These data were taken from the Oklahoma and Kansas Mesonet program. The Mesonet consists of 145 instrument platforms (as of April 2007) distributed throughout the two states. Each station measures relative humidity, wind speed and direction, air temperature, and atmospheric pressure, and reports these data as 5-min, 15-min, or half-hourly averages for the state of Oklahoma and as hourly average for the state of Kansas. Additional external data sets required by ISOLSM include the following: (1) soil type from the 1 km USGS Statsgo soils database (i.e., 20% sand, 15% silt, and 65% clay around the CF); (2) monthly mean precipitation $\delta^{18}O$ values averaged over 2–5 years of data from analyses of archived water samples collected by the EPA National Atmospheric Deposition Program (NADP) network [*Lynch et al.*, 1995] between 1980 and 1990 and interpolated across the Great Plains region [*Welker*, 2000]; and (3) the atmospheric CO_2 concentration.

[14] The model simulations also require the $\delta^{18}O$ composition of above-canopy water vapor ($\delta^{18}O_v$) and background atmospheric CO_2 ($\delta^{18}O_a$). Neither quantity is measured continuously in this region. Many factors affect $\delta^{18}O_v$ [*Lee et al.*, 2006], including evapotranspiration and horizontal and vertical atmospheric advection, and diurnal variations of up to 4‰ have been measured in this area [*Helliker et al.*, 2002; *Riley et al.*, 2003]; smaller diurnal variations (1–2‰) have been observed over temperate forests [*Lai et al.*, 2006a; *Lee et al.*, 2006]. Other investigators have shown strong linear or log linear relationships between specific humidity and $\delta^{18}O_v$ [*White and Gedzelman*, 1984; *Lee et al.*, 2006]. However, we have no information on this relationship in the SGP region, as extensive $\delta^{18}O_v$ data are not available. Instead, for this set of simulations, we set $\delta^{18}O_v$ to be in a temperature-dependent isotopic equilibrium with the most recent precipitation event [e.g., *Lee et al.*, 2006]. Although our approach only crudely captures the processes that regulate $\delta^{18}O_v$, the sensitivity of ecosystem-atmosphere $CO^{18}O$ exchanges to diurnal variations in $\delta^{18}O_v$ has been examined in detail by *Riley et al.* [2003] and found to be small, partly because the more important vapor $\delta^{18}O$ is that of within-canopy vapor, $\delta^{18}O_{cv}$, which interacts directly with $\delta^{18}O_{lw}$. *Riley et al.* [2003] also showed that diurnal variations in $\delta^{18}O_a$ can impact CO_2 isofluxes. However, since we lacked consistent diurnal measurements of $\delta^{18}O_a$, we imposed a constant value of −0.5‰, which is similar to the zonal annual mean value from midlatitude, northern hemisphere stations in the NOAA air sampling network [*Cuntz et al.*, 2003b], and is close to mean values measured 3–4 km above the surface by ARM and NOAA. There is no diagnostic solution for the canopy air space CO_2 and $CO^{18}O$ concentrations that is analogous to the H_2O and $H_2^{18}O$ solution [*Riley et al.*, 2002]. We therefore assume that canopy CO_2 and $CO^{18}O$ concentrations are the same as above-canopy values. To properly analyze potential feedbacks between leaf and canopy $CO^{18}O$ fluxes, a prognostic canopy airspace model would need to be used; to our knowledge, no previous work has addressed this issue.

2.4. Model Sensitivity Experiments

[15] Our primary objective was to better understand the effects of cloud cover and associated environmental factors such as diffuse radiation and relative humidity on ecosystem-atmosphere $CO^{18}O$ exchanges for two globally important and strongly contrasting biomes that should bracket the expected range of ecosystem responses to cloud cover: broadleaf deciduous forests and C_4 grasslands. The two types differ in photosynthetic pathway (C_3 forest and C_4 grass), life form (tree versus grass), and canopy stature (canopy heights used in ISOLSM are 20 m and 0.5 m, respectively [*Bonan*, 1996]), thereby allowing us to explore a wide range of potential ecosystem CO_2 isoflux responses to cloud cover variations.

The LAI values we used are particularly important because a higher diffuse radiation fraction is more influential with higher canopy LAI, as more leaf area is in shade during sunny conditions dominated by direct beam radiation [cf. *Roderick et al.*, 2001; *Gu et al.*, 2002; *Alton et al.*, 2005; *Knohl and Baldocchi*, 2008]. To assess the sensitivity of our results to LAI in the broadleaf forest, we ran our base simulation with the mean value (5.0) for temperate broadleaf forests from *Asner et al.* [2003]. We also ran simulations with LAI values one standard deviation above and below the mean (i.e., LAI of 3.5 and 6.5, with all other driving variables were held constant). An LAI of 6.5 is not uncommon in temperate and tropical broadleaf forests, which together contribute substantially to global primary production [e.g., *Field et al.*, 1998] and thus are particularly relevant for understanding global $\delta^{18}O_a$ variations. We set the C_4 grass canopy LAI to 3.75. This value is typical of highly productive C_4 grasslands [*Suyker and Verma*, 2001] and C_4 corn crops [*Campbell et al.*, 1999]. To assess the C_4 grass canopy LAI sensitivity, we doubled the LAI (from 3.75 to 7.5) in one simulation and reduced it by 33% (to 2.5) in another.

[16] We also tested the sensitivity of our results to shade leaf temperatures, as ISOLSM does not separately calculate the energy balance of sun and shade leaves. Shade leaves can experience a very different radiation environment than sun leaves, leading to leaf temperature gradients in the canopy [*Gu et al.*, 2002; *Larcher*, 2003]. Shade leaf temperatures can be lower than sun leaf temperatures during sunny days. We tested the impact of this difference on our results by setting forest shade leaf temperatures to canopy air temperatures. Finally, we assessed the sensitivity of our results to the uniform distribution of leaf nitrogen and photosynthetic capacity (V_{max}) between sun and shade leaves in ISOLSM. This uniformity could lead to larger shade leaf photosynthesis than would otherwise occur if these leaves become limited by Rubisco, which scales with leaf nitrogen. We halved V_{max} in forest shade leaves in a separate simulation.

3. Results and Analysis

[17] We analyzed consecutive growing season days to understand how changes in cloud cover affected the physical environment and modeled ecosystem-atmosphere CO_2 fluxes and isofluxes in a broadleaf deciduous forest canopy and a C_4 grassland canopy. Our analysis is divided into four sections to clarify the processes impacting CO_2 fluxes and isofluxes: (section 3.1) cloud cover effects on R_D/R_S, PAR, temperature, and humidity; (section 3.2) the response of photosynthesis and respiration to cloud cover; (section 3.3) the response of leaf and soil water $\delta^{18}O$ to cloud cover; and (section 3.4) the response of CO_2 isofluxes to cloud cover.

3.1. Cloud Cover Impacts on R_D/R_S and the Physical Environment

[18] During the first 3 days (DOY 193–195) of the study period, the percent of the sky obscured by thick (opaque) and thin clouds was minimal (Figure 1a). During these mostly clear days, total irradiance was high, and the PAR flux was dominated by direct beam radiation except for early in the morning and early in the evening when diffuse radiation increased (Figure 1b). In this and subsequent figures, only daytime values are plotted. These clear-sky days provided a useful basis for comparison with subsequent days (DOY 196–199), which experienced increasing thick cloud cover and midday diffuse PAR irradiance, along with reduced direct and total shortwave irradiance. The peak diffuse PAR irradiance on partly cloudy days increased more than twofold from clear days. The magnitude of midday diffuse PAR irradiance was similar to direct PAR on DOY 196, and thick cloud cover exceeded 60% for several hours. DOY 198 was by far the cloudiest day of the study period, with thick cloud cover close to 100% for much of the day (Figure 1a) and irradiance dominated by diffuse fluxes (Figure 1b). The days before and after DOY 198 were both partly cloudy, with daily maximum thick cloud cover around 60%. DOY 199 is noteworthy, as the thick and thin clouds scattered and reflected direct beam irradiance, in the process increasing the diffuse irradiance enough to produce the highest midday shortwave irradiance measured in the study period (i.e., total PAR was greater than even the clear-sky days of 193, 194, and 202). This effect of unexpectedly high midday irradiance during partly cloudy periods has been observed elsewhere [*Gu et al.*, 1999, 2001; *Urban et al.*, 2007].

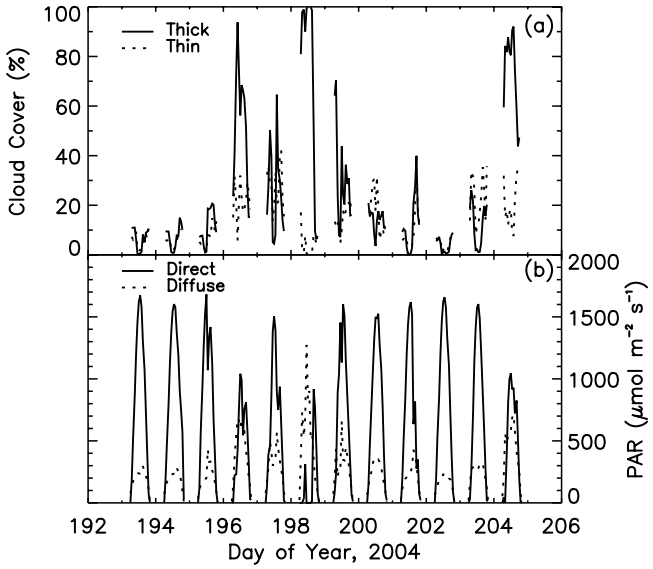

Figure 1. (a) The observed percent cover of thick (opaque) and thin clouds at the ARM Central Facility during daylight hours from DOY 193 to DOY 204 (11–22 July 2004). (b) Observed direct and diffuse PAR irradiance (μmol ‰ m^{-2} s^{-1}, using conversion factors of 4.6 μmol photons J^{-1} and 4.2 μmol photons J^{-1} for direct and diffuse radiation [*Larcher*, 2003]) on consecutive summer days (DOY 193–204) with contrasting cloud cover.

[19] The period from DOY 200–203 was mostly clear, with the lowest cloud cover of the study period measured on DOY 202 (Figure 1a). On this day, direct beam PAR was very high, about the same peak magnitude as on the other very clear day, DOY 193, but diffuse PAR was slightly lower. DOY 204 was partly to mostly cloudy (cover greater than 80% for much of the day), and it had high diffuse PAR irradiance (Figure 1b). This day preceded a heavy rain event on DOY 205. Stratifying the days by cloud cover thus produces the following classifications: clear (sunny) days (DOY 193–195, 200–203), partly cloudy days (DOY 196–197, 199, and 204), and a cloudy day (DOY 198).

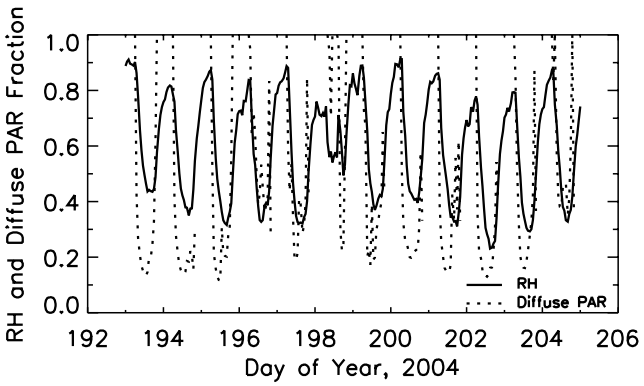

Figure 2. Observed background relative humidity (RH) and incident diffuse PAR fraction (R_D/R_S).

[20] Observed relative humidity and the diffuse PAR fraction (R_D/R_S), are shown in Figure 2. (Our analysis focuses on the observed diffuse PAR fraction, which we denote with the same notation (R_D/R_S) as the diffuse shortwave fraction following Roderick 1999; although diffuse PAR and shortwave fractions can differ slightly, during our study period they were indistinguishable from one another). Diurnal profiles of relative humidity largely followed the pattern of air temperature, and R_D/R_S followed predictable patterns on clear days with higher morning and evening values (Figure 2). Midday R_D/R_S was highest on the partly cloudy and cloudy days. Notably, the partly cloudy days (DOY 196–197, 199, and 204) did not have temperatures or humidities dramatically different from adjacent clear-sky days. Modeled leaf temperatures in the forest simulation tracked measured air temperatures, though they were higher by 1–3 K on sunny days (not shown).

[21] The increasing cloud cover during DOY 196–198 increased diffuse PAR and decreased direct and total PAR irradiance, producing a positive relationship between daytime R_D/R_S and the thick cloud cover fraction (Figure 3). Thin clouds and aerosols might also have affected R_D/R_S and contributed to some of the scatter shown in Figure 3. On partly cloudy days, midday R_D/R_S values were ~0.4, compared to ~0.15 on clear days, and the highest midday R_D/R_S occurred on DOY 198, when it reached 1.0. The strong relationship between cloud cover and R_D/R_S has been observed in a variety of other studies, and results from radiation absorption, reflection and scattering by cloud droplets.

3.2. Photosynthetic Responses to Cloud Cover Changes

3.2.1. Broadleaf Deciduous Forest

[22] The effect of cloud cover on modeled broadleaf deciduous forest canopy photosynthesis was large. Despite the lower total PAR on partly cloudy and cloudy days (DOY 196–199, 204), simulated peak canopy photosynthesis was higher on these days than on sunny days (DOY 193–195 and 200–203; Figures 1b and 4a). This enhancement was due primarily to increases in shade leaf photosynthesis from increases in diffuse PAR on these days. There were minimal changes in modeled sun leaf photosynthesis on these days because the rate was light saturated for much of the day, and even relatively large decreases in direct PAR didn't impact sun leaf photosynthesis. During these periods, sun leaf photosynthesis was limited by the amount and capacity of

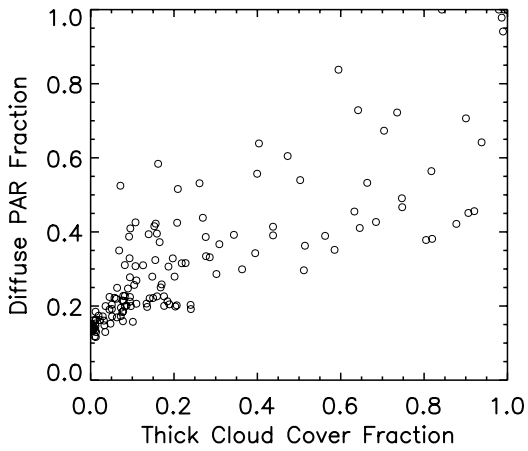

Figure 3. Observed daytime thick cloud cover fraction and incident diffuse PAR fraction (R_D/R_S) over the study period (DOY 193–204). Early morning and late afternoon values were screened to minimize the impact of low solar angles (<15°) on R_D/R_S.

the primary photosynthetic enzyme, Rubisco [i.e., *Collatz et al.*, 1991]. Also, the leaf temperature was slightly lower on the partly cloudy days compared to the sunny days because of lower radiant heating, thereby decreasing leaf respiration and photorespiration rates. The temperature sensitivity of the maximum carboxylation capacity (V_{max}) is important for sun leaf photosynthesis, as it is usually light saturated and depends directly on V_{max}, while photorespiration affects both light-limited and light-saturated rates [*Farquhar et al.*, 1980; *Collatz et al.*, 1991].

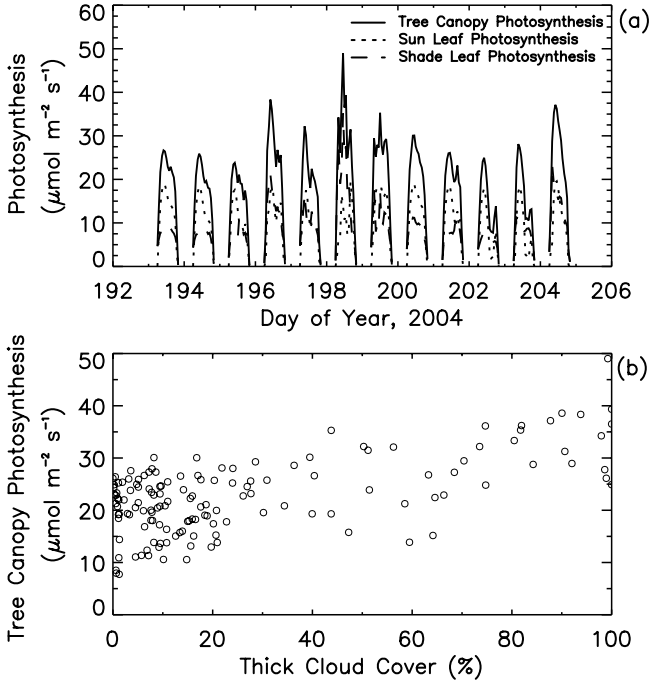

Figure 4. (a) Modeled broadleaf deciduous tree canopy photosynthesis per unit ground area (μmol m^{-2} s^{-1}) during DOY 193–204. (b) Modeled tree canopy photosynthesis (μmol m^{-2} s^{-1}) plotted against the thick cloud cover percentage for daylight hours from DOY 193 to DOY 204.

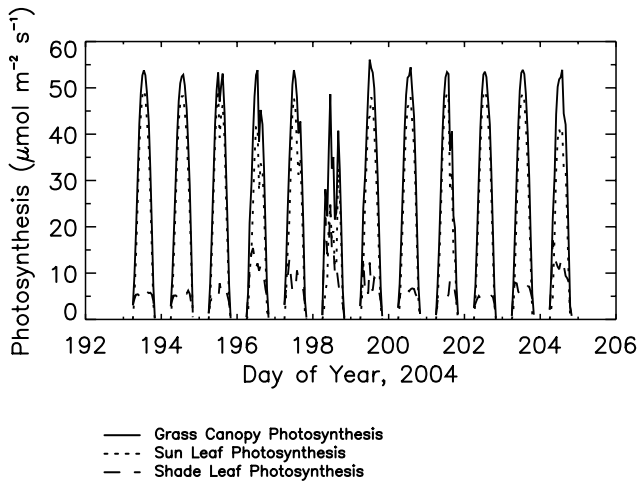

Figure 5. Modeled C_4 grass canopy photosynthesis (μmol m^{-2} s^{-1}) during DOY 193–204.

[23] In contrast to sun leaves, forest shade leaves responded strongly to the altered radiation regime induced by clouds: as cloud cover increased, diffuse PAR and shade leaf photosynthesis increased in tandem because shade leaf photosynthesis was light limited. On sunny days, peak shade leaf cumulative photosynthetic fluxes were less than half of sun leaf fluxes, whereas on partly cloudy and cloudy days the shade leaf fluxes equaled or exceeded the sun leaf values (Figure 4a). The overall positive simulated forest canopy photosynthetic response to increasing cloud cover (slope 0.15, r^2 = 0.37; Figure 4b) thus resulted primarily from increased shade leaf carbon uptake with increased R_D/R_S.

3.2.2. C_4 Grassland

[24] The C_4 grass canopy photosynthetic response to cloud variations was opposite that of the broadleaf deciduous forest canopy: increasing cloud cover generally led to decreased canopy photosynthesis. The negative response of C_4 photosynthesis to increasing R_D/R_S was stronger than its response to cloud cover (not shown). Although grass shade leaf photosynthesis responded positively to increased cloud cover due to increased diffuse PAR, sun leaf photosynthesis responded negatively to the decrease in direct beam radiation, and sun leaf photosynthesis was much larger than shade leaf photosynthesis during almost all cloud cover conditions (Figure 5).

[25] The modeled C_4 grass canopy photosynthesis closely followed daily irradiance patterns, in agreement with leaf and canopy-scale observations for C_4 plants [*Suyker and Verma*, 2001; *Larcher*, 2003]. In general, the highest predicted C_4 grass canopy photosynthesis rates occurred during the clear-sky days (DOY 193–195, 200–203), and the lowest rates occurred during the cloudiest days (DOY 196, 198, 204). The one important exception (on DOY 199, which was partly cloudy) proves the rule: peak insolation values on this day were the highest of the study period because of cloud scattering and reflection, and modeled peak C_4 grass photosynthesis was also highest on this day (Figure 5). Modeled peak canopy photosynthesis was large because of the high LAI values we imposed, although there are examples of well-watered and fertilized natural C_4 grassland and C_4 crop canopies exhibiting even higher productivity [*Piedade et al.*, 1991; *Jones*, 1992; *Morison et al.*, 2000]. The net ecosystem exchange (NEE) values predicted by ISOLSM (not shown) ranged from −15 to −35 μmol m^{-2} s^{-1}, similar to NEE measured in a C_4 grass-dominated pasture in this region [*Suyker and Verma*, 2001].

[26] The fundamentally different response to cloud cover of the C_4 grass canopy (as opposed to the forest canopy) was at least partly due to canopy stature and the lower effective shade leaf area (and higher effective sun leaf area) in the much shorter grass canopy. Grass leaves have a more vertical orientation (erectophile morphology), and broadleaf deciduous tree leaves have a more horizontal orientation, so that at high solar angles the sun leaf area in grass canopies is higher than the comparable sun leaf area of broadleaf deciduous tree canopies [*Jones*, 1992; *Larcher*, 2003]. Another reason for the different response to irradiance is that both sun and shade leaf photosynthetic rates are almost always limited by light in the C_4 grass simulation. A hallmark of C_4 plants is their dominance in high-light and high-temperature environments such as grasslands and savannas [*Long*, 1999; *Sage et al.*, 1999]. Photosynthesis in unstressed C_4 plants does not saturate on sunny days, unlike the typical light saturation for C_3 plants [*Collatz et al.*, 1991, 1992].

[27] The decline in C_4 grass canopy photosynthesis with increasing cloud cover and R_D/R_S parallels the empirical results from eddy flux studies assessed by *Niyogi et al.* [2004], who found that increasing aerosol optical depth increased R_D/R_S and reduced R_S. This led to increases in net carbon uptake by C_3 ecosystems, but strong reductions in net carbon uptake for a C_4 natural grassland. Although not explicitly a response to cloud cover variations per se, this study supports our modeling results: increasing R_D/R_S and decreasing R_S reduces C_4 photosynthesis, without the diffuse light photosynthetic enhancement often seen in C_3 canopies. Our predictions also agree with *Turner et al.* [2003], who studied the relationship between measured gross primary production (GPP) and absorbed PAR in a cross-biome comparison. The C_4-dominated tallgrass prairie displayed a nearly linear relationship between GPP and APAR, unlike other biomes, which exhibited more typical light saturation responses (i.e., a hyperbolic relationship between GPP and APAR). Thus, decreases in R_S and increases in R_D/R_S, whether caused by clouds or aerosols, should decrease GPP in C_4 grasses, but not necessarily in C_3 plants.

3.2.3. Response of Canopy Light Use Efficiency to Cloud Cover and R_D/R_S Variations

[28] The response of forest photosynthesis to cloud cover and irradiance is related to how efficiently the canopy converts solar radiation to chemical energy, a quantity referred to as gross or GPP light use efficiency (LUE) (mol CO_2 mol^{-1} APAR). The broadleaf deciduous forest gross LUE was inversely proportional to irradiance. Indeed, the forest canopy strongly increased its gross LUE as R_D/R_S increased (Figure 6a). The daily averaged forest gross LUE for clear/sunny days (DOY 193–195, 200–203) was 0.031 mol CO_2 mol^{-1} APAR, for partly cloud days (DOY 196–197, 199, 204) was 0.038 mol CO_2 mol^{-1} APAR, and for the cloudy day (DOY 198) was 0.048 mol CO_2 mol^{-1} APAR. This pattern follows the expectations of increasing LUE with increasing cloud cover and R_D/R_S demonstrated previously in eddy flux [e.g., *Hollinger et al.*, 1994; *Gu et al.*, 2002; *Rocha et al.*, 2004; *Min*, 2005] and modeling [*Norman*

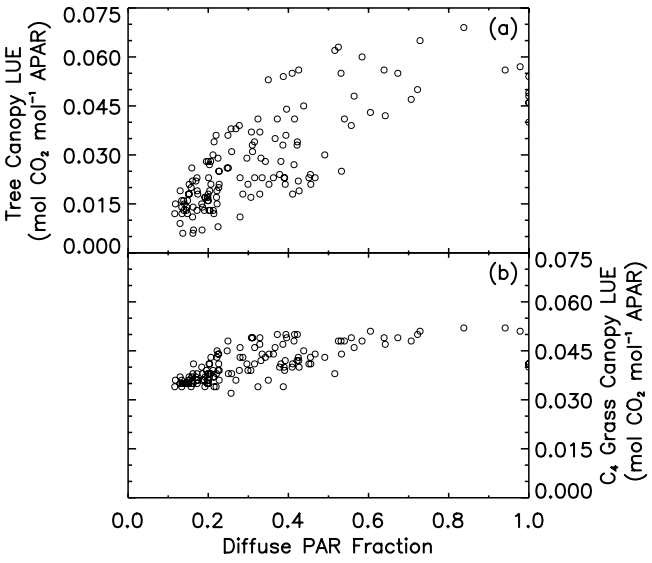

Figure 6. (a) Modeled gross LUE (mol CO_2 mol^{-1} APAR) in the broadleaf deciduous tree canopy plotted against observed R_D/R_S during daylight hours (solar angles >15°). (b) Modeled C_4 grass canopy gross LUE (mol CO_2 mol^{-1} APAR) plotted against observed R_D/R_S during daylight hours.

and Arkebauer, 1991; *Choudhury*, 2001] studies. The increase of LUE with R_D/R_S depends on canopy structure and openness [*Alton et al.*, 2005], and, as we show below, on photosynthetic pathway.

[29] During periods of high R_D/R_S, both sun and shade leaves in the forest were light limited and thus displayed a linear response to APAR. The linear slope between photosynthesis and APAR is defined as the quantum yield of photosynthesis [*Larcher*, 2003]. In C_3 plants the highest intrinsic quantum yield is ~0.085 mol CO_2 mol^{-1} incident PAR, and its temperature sensitivity is largely driven by photorespiration [*Collatz et al.*, 1998; *Ehleringer et al.*, 1997]. Therefore, canopy LUE under low light closely follows the temperature-dependent photorespiration rate. Forest LUE values reached their lowest values around midday when sun leaves were light saturated and leaf temperatures were high. Forest canopy LUE dropped nonlinearly with temperature and reached its lowest values on the sunniest, hottest days when R_D/R_S was lowest (Figure 6a).

[30] The C_4 canopy maintained high gross LUE over the study period, and was relatively insensitive to variations in cloud cover, irradiance, and leaf temperature. Since C_4 sun and shade leaf photosynthesis was almost always light limited, the relationship between canopy photosynthesis and APAR was linear across the entire PAR range, and thus canopy LUE was very close to the leaf quantum yield. The intrinsic modeled leaf C_4 quantum yield is 0.06 mol CO_2 mol^{-1} incident PAR [*Collatz et al.*, 1998], although natural C_4 monocots can occasionally exceed this value [*Ehleringer et al.*, 1997]. C_4 plants typically maintain nearly constant quantum yields across a range of temperatures under low-light conditions [*Ehleringer et al.*, 1997; *Collatz et al.*, 1998]. During most daytime hours of the study period, the C_4 grass canopy LUE varied from ~0.035–0.05 mol CO_2 mol^{-1} APAR, and, unlike the forest canopy, there was no consistent relationship with cloud cover or leaf temperature. There was a relationship with R_D/R_S, although it was weak compared with the forest LUE response to R_D/R_S (Figures 6a and 6b).

3.3. Leaf and Soil Water $\delta^{18}O$ Responses to Cloud Cover Changes

[31] The simplest formulation for leaf water $\delta^{18}O$ is captured in the steady state prediction for $\delta^{18}O$ of an evaporating surface, in this case within leaves [*Craig and Gordon*, 1965; *Farquhar et al.*, 1989; *Yakir and Sternberg*, 2000]:

$$\delta^{18}O_{lws} = \delta^{18}O_{xy} + \varepsilon_k + \varepsilon^* + \left(\delta^{18}O_{cv} - \varepsilon_k - \delta^{18}O_{xy}\right)\frac{e_a}{e_i}. \quad (1)$$

In this equation, $\delta^{18}O_{xy}$ and $\delta^{18}O_{cv}$ are the $^{18}O/^{16}O$ composition of stem xylem (source) water and within-canopy atmospheric water vapor; ε_k is the weighted mean of kinetic fractionations against $H_2^{18}O$ molecules diffusing through the stomata and across the leaf boundary layer (32 and 21‰, respectively [*Cappa et al.*, 2003]); ε^* is the equilibrium fractionation between liquid and vapor phases over a saturated surface (~9.4‰ at 298K [*Horita and Wesolowski*, 1994]); and e_a and e_i are the water vapor pressures (Pa) in the canopy atmosphere and inside leaf stomata, respectively.

[32] Bulk leaf water $\delta^{18}O$ is often not accurately represented by a steady state formulation [*Dongmann et al.*, 1974; *Zundel et al.*, 1978; *Wang et al.*, 1998; *Harwood et al.*, 1998; *Cernusak et al.*, 2002; *Cuntz et al.*, 2003a; *Barbour et al.*, 2004; *Farquhar and Cernusak*, 2005; *Cernusak et al.*, 2005; *Seibt et al.*, 2006]. *Dongmann et al.* [1974] first proposed a nonsteady state leaf water model; our treatment in ISOLSM follows closely from their work, and describes the change in leaf water $\delta^{18}O$ as an asymptotic approach to a steady state value. The nonsteady state leaf water $\delta^{18}O$ at time t (i.e., $\delta^{18}O_{lw}$ (t)) is calculated implicitly from the steady state estimate ($\delta^{18}O_{lws}(t)$) and the nonsteady state $\delta^{18}O_{lw}$ (i.e., $\delta^{18}O_{lw}$ $(t-1)$) from the previous time step as follows:

$$\delta^{18}O_{lw}(t) = e^{\frac{-\Delta t}{\tau}}\delta^{18}O_{lw}(t-1) + \left(1 - e^{\frac{-\Delta t}{\tau}}\right)\delta^{18}O_{lws}(t). \quad (2)$$

Here, τ is the leaf water time constant (s) and in practice Δt is the model time step (s). τ is calculated separately for sun and shade leaves as the ratio between the leaf stock of water interacting with transpiration (M_l) and the gross water vapor flux out of leaves:

$$\tau = \frac{M_l}{\left(\frac{e_i}{RT_v}\right)g_s}. \quad (3)$$

Here, R is the universal gas constant (8.314 J mol^{-1} K^{-1}), T_v is vegetation temperature (K), and g_s is stomatal conductance (sun or shade leaf, m s^{-1}). The leaf water content, M_l, of both sun and shade leaves is set to a constant value of 10 mol m^{-2}, which is consistent with limited available observations from a temperate needleleaf forest [*Seibt et al.*, 2006] and a tropical broadleaf forest [*Förstel*, 1978]. In reality, the water content of the average shade leaf is undoubtedly different from the average sun leaf, since there are well-known differences in specific leaf area between sun and shade leaves [*Chapin et al.*, 2002; *Larcher*, 2003]. However, we lacked data to reliably

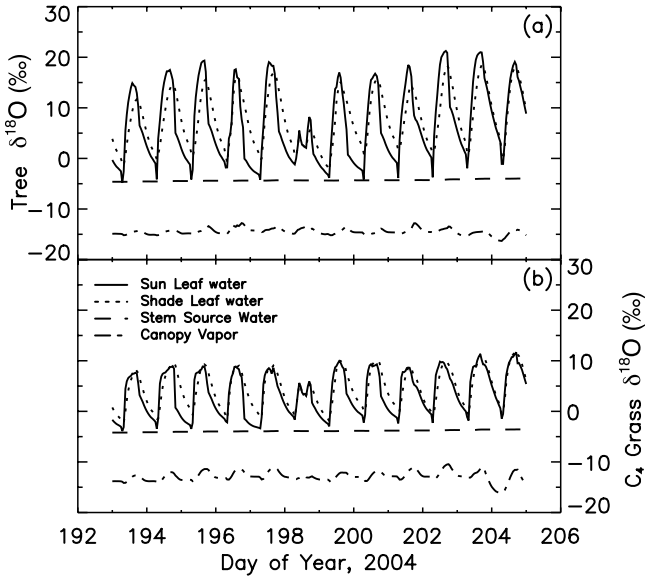

Figure 7. (a) Shown is δ^{18}O (‰, relative to VSMOW) of leaf water ($\delta^{18}O_{lw}$) for sun and shade leaves and stem source water ($\delta^{18}O_{xy}$) and canopy vapor ($\delta^{18}O_{cv}$) in the broadleaf deciduous forest canopy simulation. (b) The same quantities plotted for the C_4 grass canopy simulation.

and accurately set this difference and assumed a constant value in both biomes and leaf types.

3.3.1. Broadleaf Deciduous Forest

[33] Simulated nonsteady $\delta^{18}O_{lw}$ for forest sun and shade leaves varied by over 20‰ during the study period (Figure 7a: all δ^{18}O-H_2O values are reported relative to the Vienna SMOW (VSMOW) scale). The diurnal cycle of $\delta^{18}O_{lw}$ for sun and shade leaves was inversely related to canopy relative humidity. Assuming steady state and no leaf boundary layer fractionation, the change in δ^{18}O of an evaporating leaf at steady state will be roughly −0.4‰ for each percent change in relative humidity [*Craig and Gordon*, 1965]. This slope will be slightly smaller when including isotopic fractionation across the leaf boundary layer and nonsteady state effects. Over the study period, the slope of the linear regression for daytime sun leaf $\delta^{18}O_{lw}$ versus canopy relative humidity was −0.39‰ per % change in relative humidity. By contrast, the slope for shade leaves was lower, approximately −0.28‰ per % change in relative humidity. $\delta^{18}O_{cv}$ varied diurnally between −13‰ and −16‰ in response to canopy transpiration, soil evaporation, and exchange with above-canopy air. This variation was dampened by a 3-h canopy turnover time imposed to account for turbulent air mass exchange between the canopy and atmosphere [*Riley et al.*, 2002].

[34] The sun and shade $\delta^{18}O_{lw}$ differed from the steady state ($\delta^{18}O_{lws}$) and from each other during most of the day (both leaves had the same water content, were at the same temperature, and were exposed to the same canopy vapor pressure and isotopic composition). This difference occurs because the leaf water time constant depends on the stomatal conductance of each leaf type (equation (3)), which is linked to the photosynthetic rate. For much of the day, sun leaf $\delta^{18}O_{lw}$ was close to steady state. Shade leaf $\delta^{18}O_{lw}$ generally lagged sun leaf $\delta^{18}O_{lw}$, with smaller lags on partly cloudy and cloudy days when shade leaf photosynthesis and transpiration were higher because of enhanced diffuse PAR (e.g., DOY 196, 204). Both sun and shade leaves remained elevated above source stem water, especially in the early evening and through much of the night.

[35] As is apparent from $\delta^{18}O_{xy}$ (Figure 7a), variation in modeled soil water δ^{18}O ($\delta^{18}O_{sw}$) was minimal across the study period. Even in the upper soil layers where $\delta^{18}O_{sw}$ can strongly increase because of evaporative enrichment [*Allison et al.*, 1983; *Riley*, 2005], $\delta^{18}O_{sw}$ did not vary greatly because transpiration dominated evapotranspiration in these high-LAI simulations. The magnitude and variability of soil-respired CO_2 isofluxes was fairly minimal, in agreement with earlier Great Plains modeling studies [*Riley et al.*, 2002, 2003; *Lai et al.*, 2006a; *Still et al.*, 2005], and will not be discussed further.

3.3.2. C_4 Grassland

[36] There was an unanticipated difference between the broadleaf forest and C_4 grassland $\delta^{18}O_{lw}$, with peak C_4 grassland $\delta^{18}O_{lw}$ over the period never exceeding 12‰, whereas peak forest $\delta^{18}O_{lw}$ routinely exceeded 18‰ (Figures 7a and 7b), despite identical precipitation δ^{18}O, radiation, and meteorological forcing (including above-canopy relative humidity). The difference is due to feedbacks between transpiration and within-canopy relative humidity. The canopy relative humidity (not shown) was substantially higher in the C_4 grassland. Canopy relative humidity is calculated in ISOLSM from the canopy temperature and vapor pressure, which depends on exchanges with background vapor pressure, as well as transpiration and soil and canopy evaporation. The canopy relative humidity in the C_4 grassland simulation never dropped below 55% over the study period, whereas modeled canopy relative humidity in the broadleaf forest was only slightly elevated from the measured above-canopy humidity, reaching values below 40% near midday. The higher average daytime relative humidity in the C_4 canopy (relative to the broadleaf forest canopy) depleted $\delta^{18}O_{lw}$.

[37] The higher relative humidity in the C_4 canopy was due to higher transpiration fluxes. Although C_4 plants typically exhibit water use efficiencies roughly twice those of comparable C_3 plants [*Pearcy and Ehleringer*, 1984], this difference was overcome by much higher photosynthetic fluxes in the C_4 grass canopy compared to the forest canopy (Figures 4a and 5). The higher relative humidity in the C_4 grass canopy was also due to a lower aerodynamic conductance between the grass canopy and overlying atmosphere compared to the taller and aerodynamically rougher forest, leading to a greater offset between the canopy relative humidity and the background atmosphere. The effect of these differences is also apparent in the greater diurnal cycle of canopy vapor δ^{18}O ($\delta^{18}O_{cv}$) in the C_4 grassland (Figure 7b), as it was more strongly influenced by transpiration. The greater diurnal cycle in $\delta^{18}O_{cv}$ also contributed to the transpiration feedback on $\delta^{18}O_{lw}$, although the feedback was primarily due to the change in canopy relative humidity.

3.4. Response of Photosynthetic Isofluxes to Cloud Cover and R_D/R_S

[38] Leaf CO_2 isofluxes depend on both photosynthesis and discrimination against $CO^{18}O$. Discrimination against $CO^{18}O$ ($^{18}\Delta$) depends upon the δ^{18}O value of CO_2 in equilibrium with H_2O inside leaf chloroplasts ($\delta^{18}O_c$) and the ratio of chloroplast CO_2 to atmospheric CO_2 concentrations

(C_c/C_a). Gaseous CO_2 equilibrates with liquid water in the mesophyll cells lining the bottom of the stomatal pore via the activity of the carbonic anhydrase enzyme. This equilibration labels CO_2 with the isotopic signature of leaf water plus an equilibrium offset [*Farquhar and Lloyd*, 1993; *Farquhar et al.*, 1993; *Gillon and Yakir*, 2000; *Affek et al.*, 2005], and has been shown to be lower in C_4 grasses [*Gillon and Yakir*, 2001]. The discrimination can be estimated as [*Farquhar and Lloyd*, 1993; *Farquhar et al.*, 1993; *Ciais et al.*, 1997a; *Gillon and Yakir*, 2000; *Yakir and Sternberg*, 2000]

$$^{18}\Delta = \varepsilon_d + \frac{C_c}{C_a - C_c}\left(\delta^{18}O_c - \delta^{18}O_a\right). \quad (4)$$

ε_d is the weighted kinetic fractionation accompanying diffusion of $CO^{18}O$ molecules across the stomata, boundary layer, and the mesophyll walls (~7.4‰ [*Farquhar and Lloyd*, 1993; *Gillon and Yakir*, 2001]), $\delta^{18}O_c$ is calculated from $\delta^{18}O_{lw}$ and a temperature-dependent fractionation factor [*Brenninkmeier et al.*, 1983], and $\delta^{18}O_a$ is the $\delta^{18}O$ value of background atmospheric CO_2. The $\frac{C_c}{C_a - C_c}$ term arises from mass balance of $CO^{18}O$ molecules, and when multiplied by net leaf uptake, quantifies the back diffusion or retro-diffusion flux of CO_2 molecules, which have a different $\delta^{18}O$ from when they entered the leaf. This change occurs because only some of the CO_2 entering the leaf is fixed by photosynthesis, while the remainder diffuses out after full or partial isotopic equilibration with leaf water [*Farquhar et al.*, 1993; *Flanagan et al.*, 1994; *Gillon and Yakir*, 2001].

[39] These bidirectional fluxes, termed F_{al} (atmosphere-to-leaf) and F_{la} (leaf-to-atmosphere), together sum to net photosynthesis, A_{net} (which includes leaf respiration). Each of these global fluxes (roughly 300 and 200 Pg C a^{-1} for F_{al} and F_{la}, respectively [*Ciais et al.*, 1997a]) is larger than any other carbon flux term in the contemporary carbon budget. Equation (4) can be recast as a function of F_{al} and F_{la}:

$$^{18}\Delta = \frac{F_{la}}{A_{net}}\left(\delta^{18}O_c - \varepsilon_d - \delta^{18}O_a\right) + \frac{F_{al}}{A_{net}}\varepsilon_d. \quad (5)$$

[40] The first, right-hand side term captures the effective discrimination associated with the return, or retro-diffused, flux from leaves, and its sign and magnitude vary directly with changes in $\delta^{18}O_c$. The combined net photosynthetic isoflux, in units of μmol ‰ m^{-2} s^{-1}, is the product of photosynthetic discrimination ($^{18}\Delta$) and net leaf photosynthesis (A_{net}):

$$A_{net}\ ^{18}\Delta = F_{la}\left(\delta^{18}O_c - \varepsilon_d - \delta^{18}O_a\right) + F_{al}\varepsilon_d = {}^{18}F_{la} + {}^{18}F_{al}. \quad (6)$$

[41] Bidirectional CO_2 isofluxes across leaf stomata can occur during nighttime periods [e.g., *Cernusak et al.*, 2004; *Barbour et al.*, 2007]. Although this effect is potentially important, accurate quantification requires a model with a canopy air space and prognostic calculations of CO_2 and $CO^{18}O$ concentrations throughout the night [e.g., *Seibt et al.*, 2006], along with a model that accurately predicts stomatal conductance and the concentration of CO_2 in the substomatal air spaces (C_i) and inside leaf chloroplasts (C_c) when photosynthesis is zero. For this study, we focused on daytime isofluxes only.

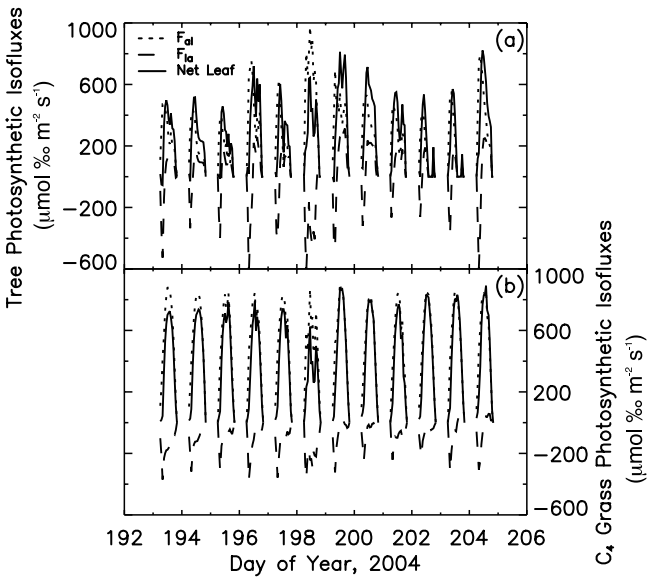

Figure 8. (a) Modeled photosynthetic isofluxes (μmol ‰ m^{-2} s^{-1}), ${}^{18}F_{al}$ and ${}^{18}F_{la}$, and their sum ($A_{net}{}^{18}\Delta$) for the broadleaf tree canopy. (b) The same quantities plotted for the C_4 grass canopy.

3.4.1. Broadleaf Deciduous Forest

[42] The $^{18}\Delta$ diurnal cycle (not shown) was strongly related to $\delta^{18}O_{lw}$ enrichment as canopy relative humidity declined with increasing air temperature. There was a decline in $^{18}\Delta$ with increasing cloud cover that followed from a small decrease in $\delta^{18}O_{lw}$ on partly cloudy days, and a large decrease in $\delta^{18}O_{lw}$ on the cloudy day (Figures 1a and 7a). Neither C_c nor leaf temperature (the other components of $^{18}\Delta$) varied appreciably with cloud cover for either leaf type. The bidirectional leaf CO_2 fluxes, F_{al} and F_{la}, varied diurnally with photosynthesis and increased strongly with cloud cover, particularly for shade leaves. The ${}^{18}F_{al}$ and ${}^{18}F_{la}$ isofluxes were often in opposition: the gross flux into stomata (${}^{18}F_{al}$) always enriched atmospheric $\delta^{18}O_a$ (i.e., was always positive in δ notation), whereas the retro-diffused flux (${}^{18}F_{la}$) depleted $\delta^{18}O_a$ in the morning (i.e., a negative isoflux) and enriched it in the afternoon (Figure 8a). The early morning depletion occurred because $\delta^{18}O_{lw}$ (and thus $\delta^{18}O_c$) was relatively depleted from the previous night when it approached $\delta^{18}O_{xy}$ (Figure 7a); also, early morning canopy relative humidity was still high, and the transpiration flux was reduced because of low light levels, thus affecting the leaf water time constant. At this site, where we imposed a fixed $\delta^{18}O_a$ consistent with the measured annual zonal mean (−0.5‰), $\delta^{18}O_c$ must exceed ~7.0‰ before the retro-diffused isoflux (${}^{18}F_{la}$) has a positive isotopic forcing (i.e., enriches $\delta^{18}O_a$).

[43] As relative humidity decreased in the late morning, $\delta^{18}O_c$ became more enriched until it exceeded the ~7‰ threshold and the leaf-to-atmosphere isoflux (${}^{18}F_{la}$) reinforced the atmosphere-to-leaf isoflux (${}^{18}F_{al}$). The forest sun leaf $\delta^{18}O_{lw}$ corresponding to this $\delta^{18}O_c$ threshold occurred at a canopy relative humidity of ~60%. Only on the cloudiest

and coolest day (DOY 198) did $\delta^{18}O_{lw}$ stay below this value throughout the day (Figures 7a and 8a). The greatest $\delta^{18}O_{lw}$ enrichment occurred on the sunniest, hottest day when canopy relative humidity was lowest (DOY 202), and ${}^{18}F_{la}$ was mostly positive. Because of high leaf temperatures on DOY 202, however, A_{net} and net leaf isofluxes ($A_{net}{}^{18}\Delta$ or ${}^{18}F_{al} + {}^{18}F_{la}$) were lowest of the study period.

[44] If $\delta^{18}O_{lw}$ and $\delta^{18}O_c$ are sufficiently negative, the net leaf isoflux can deplete $\delta^{18}O_a$. The $\delta^{18}O_c$ where negative net photosynthetic isotope fluxes (${}^{18}F_{al} + {}^{18}F_{la} < 0$) occur is a function of $\delta^{18}O_a$, the C_c/C_a ratio, and ε_d. $\delta^{18}O_c$ values more depleted than approximately −4.2‰ caused net forest photosynthetic isofluxes to be negative. During the 12-day study period, negative CO_2 isofluxes occurred only briefly on DOY 193 when $\delta^{18}O_{lw}$ approached $\delta^{18}O_{xy}$ and photosynthesis was just beginning (Figure 8a). Because the $\delta^{18}O$ of growing season precipitation is rarely more depleted than −5‰ at these latitudes [*Welker*, 2000; *Bowen and Wilkinson*, 2002], forest photosynthetic isofluxes will almost always enrich $\delta^{18}O_a$. At higher latitudes where precipitation $\delta^{18}O$ is lower, leaf CO_2 isofluxes can deplete $\delta^{18}O_a$ [e.g., *Francey and Tans*, 1987; *Farquhar et al.*, 1993; *Ciais et al.*, 1997b], because of ${}^{18}F_{la}$ outweighing ${}^{18}F_{al}$.

[45] The net photosynthetic isoflux ($A_{net}{}^{18}\Delta$, solid line in Figure 8a) generally followed the daily variations in canopy photosynthesis (Figure 4a), with larger isofluxes on partly cloudy days (DOY 196–197, 199, 204) than on clear, sunny days (DOY 193–195, 201–203), an effect driven by shade leaves. However, the cloudy day (DOY 198) exhibited intermediate CO_2 isofluxes: although it had the largest peak photosynthesis, this was countered by the lowest $\delta^{18}O_{lw}$ and ${}^{18}\Delta$ of the study period (Figures 4a, 7a, and 8a). Partitioning the net leaf isoflux ($A_{net}{}^{18}\Delta$) into ${}^{18}F_{al}$ and ${}^{18}F_{la}$ (equation (6)) reveals the canopy response to cloud cover in more detail. The ${}^{18}F_{al}$ isoflux increased strongly with increasing cloud cover because of an increase in shade leaf and canopy photosynthesis with cloud cover. By contrast, ${}^{18}F_{la}$ did not exhibit a strong relationship with cloud cover during daytime hours of the study period. Indeed, both negative and positive ${}^{18}F_{la}$ values occurred for a range of cloud cover, as $\delta^{18}O_{lw}$ and thus $\delta^{18}O_c$ alternated from relatively depleted values in the morning to enriched values in the afternoon after they crossed the ∼7.0‰ threshold. Thus, for the sum of ${}^{18}F_{al}$ and ${}^{18}F_{la}$ (i.e., $A_{net}{}^{18}\Delta$), no clear response to cloud cover occurred. When net photosynthetic isofluxes are plotted against R_D/R_S, however, there was a weak negative relationship, with the highest isofluxes centered at an R_D of ∼0.4. This was driven by ${}^{18}F_{la}$, which peaked around this value in our simulations; at R_D/R_S values above ∼0.6, ${}^{18}F_{la}$ was always negative. The peak isoflux at an R_D/R_S of 0.4 was not driven solely by photosynthetic responses to diffuse irradiance, as peak canopy photosynthesis occurred at higher R_D/R_S values. Rather, it was the combination of enhanced photosynthesis with higher $\delta^{18}O_{lw}$ due to lower canopy relative humidity at this particular R_D/R_S. These conditions occurred around midday on the partly cloudy days (DOY 196, 199, 204) that have the largest peak and cumulative daily isofluxes.

3.4.2. C_4 Grassland

[46] There were large differences in leaf isofluxes between the forest and C_4 grassland simulations that arose from differences in the internal CO_2 concentrations between these different physiological types, as well as differences in their $\delta^{18}O_c$ values (section 3.3). Comparing chloroplast CO_2 concentrations between C_3 and C_4 plants is difficult since the C_4 pathway concentrates CO_2 around Rubisco in the bundle sheath cell chloroplasts, and raises CO_2 concentrations to much higher levels than occur in mesophyll cell chloroplasts of C_3 plants [*von Caemmerer and Furbank*, 2003]. For these simulations, we used the C_i value calculated in ISOLSM. Typical C_i/C_a ratios for C_4 plants range from 0.2 to 0.4, whereas those for most C_3 plants are 0.6–0.8 [*Pearcy and Ehleringer*, 1984; *Collatz et al.*, 1991, 1992]. At similar photosynthetic rates, F_{la} can be much higher in C_3 than C_4 plants [*Still et al.*, 2005; *Hoag et al.*, 2005]. For example, a C_i/C_a ratio of 0.8 produces a F_{la} four times larger than a ratio of 0.2 produces for the same net leaf flux.

[47] The C_4 grass photosynthetic isoflux, dominated by ${}^{18}F_{al}$ from sun leaves, is almost always larger and less variable than the forest isoflux (Figure 8b). However, ${}^{18}F_{la}$ is smaller in the grass than in the forest, and it remains negative throughout the day and never reinforces ${}^{18}F_{al}$, except for three brief periods on DOY 199, 203, and 204 (Figures 8a and 8b). This negative isotopic forcing on the atmosphere is due to the lower $\delta^{18}O_{lw}$ (Figures 7a and 7b) and the larger ε_d in the C_4 grass simulation. $\delta^{18}O_c$ must exceed a threshold value of ∼7.9‰ before the ${}^{18}F_{la}$ from C_4 plants has a positive isotopic forcing on the atmosphere. However, because leaf temperatures exceeded 30°C on the days with highest $\delta^{18}O_{lw}$ (DOY 199, 200, 202), and the CO_2-H_2O fractionation has a sensitivity of −0.2‰ K^{-1} [*Brenninkmeier et al.*, 1983; *Ciais et al.*, 1997a], ${}^{18}F_{la}$ is almost always negative during the study period (Figure 8b).

[48] Because the magnitude of ${}^{18}F_{la}$ will be much smaller in C_4 plants compared to C_3 plants because of lower C_i/C_a ratios [*Still et al.*, 2005] and reduced equilibration between CO_2 and H_2O from lower carbonic anhydrase activity [*Gillon and Yakir*, 2001], photosynthesis by C_4 plants will almost always enrich $\delta^{18}O_a$. The positive isotopic forcing associated with ${}^{18}F_{al}$ will in almost every case be much larger than the negative isotopic forcing from ${}^{18}F_{la}$. Because C_4 plants are largely restricted to tropical and subtropical savannas and grasslands [*Still et al.*, 2003], the $\delta^{18}O$ of precipitation and thus of plant xylem water ($\delta^{18}O_{xy}$), is relatively enriched [*Bowen and Wilkinson*, 2002]. For example, *Ometto et al.* [2005] measured Amazonian C_4 pasture grasses with $\delta^{18}O_{xy}$ values between −3‰ and −9‰, and mean values around −5‰. These values, and measurements from C_4-dominated tallgrass prairies in Oklahoma and Kansas [*Helliker et al.*, 2002; *Riley et al.*, 2003; *Lai et al.*, 2006b], are similar to the mean predicted $\delta^{18}O_{xy}$ at our site (Figure 7). Given a typical midday C_4 plant C_i/C_a ratio of 0.3 and assuming complete equilibration, $\delta^{18}O_c$ at this site would have to be below approximately −17.3‰ for net C_4 photosynthetic isofluxes to deplete $\delta^{18}O_a$. Using precipitation $\delta^{18}O$ regressions from *Bowen and Wilkinson* [2002], $\delta^{18}O_{lw}$ and thus $\delta^{18}O_c$ values that are sufficiently depleted occur above ∼60°N. Although C_4 plants do grow north of 50° N [e.g., *Schwarz and Redmann*, 1988; *Beale and Long*, 1995], they are uncommon and do not substantially affect regional carbon fluxes.

[49] While C_4 canopy photosynthesis decreased slightly with increasing cloud cover, net photosynthetic isofluxes ($A_{net}{}^{18}\Delta$) exhibited no clear relationship with cloud cover. ${}^{18}\Delta$ did not vary with cloud cover, as an increase in the F_{al} component of ${}^{18}\Delta$ due to an increase in C_c with cloud cover

was countered by a decrease in the F_{la} component of $^{18}\Delta$ driven by the slight decrease of $\delta^{18}O_{lw}$ and $\delta^{18}O_c$ with cloud cover. Over the study period, the flux-weighted mean C_4 grassland canopy $^{18}\Delta$ was ~12‰, with ~2/3 of this from ε_d. There was a weak negative response of $A_{net}{}^{18}\Delta$ to increasing R_D/R_S, just as there was between C_4 canopy photosynthesis and R_D/R_S. In both cases, peak uptake occurred at R_D/R_S values between 0.2 and 0.4, and declined sharply above 0.4. There was a strong positive relationship (slope = 0.46; r^2 = 0.89) between the net C_4 photosynthetic isoflux and incident PAR (i.e., the canopy isotope light response curve; Figure 9).

3.5. Sensitivity to Leaf Area Index

3.5.1. Broadleaf Deciduous Forest

[50] We examined the sensitivity of our results to LAI given the importance of this canopy characteristic in the response to clouds and R_D/R_S as highlighted by earlier studies [e.g., *Rocha et al.*, 2004; *Urban et al.*, 2007; *Knohl and Baldocchi*, 2008]. We altered LAI values throughout the study period, with other model driving data unchanged from control simulations. Relative to the control, forest canopy photosynthesis and transpiration declined in the low-LAI simulation and increased in the high-LAI one, driven by the shade leaf response. The changes in canopy transpiration lowered or raised canopy relative humidity by a few percent relative to the base case. The impact of changing LAI on canopy relative humidity and $\delta^{18}O_{lw}$ was most dramatic on the cloudy day (DOY 198) when R_D/R_S and diffuse PAR were highest. This day exhibited the highest peak shade leaf and canopy photosynthesis in the base LAI simulation, and also the greatest humidification of the canopy from transpiration (since wind speed and exchange with the atmosphere was not different from adjacent days). On DOY 198, peak daytime steady state $\delta^{18}O_{lw}$ values were raised by 1.4‰ in the low-LAI (3.5) simulation relative to the base case, and lowered by 0.3‰ in the high-LAI (6.5) simulation.

[51] Taken in isolation, this transpiration feedback on $\delta^{18}O_{lw}$ would increase (decrease) $^{18}\Delta$ in the lower- (higher-) LAI simulations. However, the retroflux scalar (equation (4)) was lowered in the reduced LAI simulation as the relative contribution of shade leaves with slightly higher C_c values declined relative to the base LAI. The effect of these differences was to quantitatively reduce the importance of $^{18}F_{la}$ in the reduced LAI simulations, and as a result, net photosynthetic isofluxes ($A_{net}{}^{18}\Delta$) were more dominated by $^{18}F_{al}$. Because $^{18}F_{al}$ scales with leaf photosynthesis and is unaffected by $\delta^{18}O_{lw}$, it exhibited a positive correlation with cloud cover; as LAI was reduced, a coherent relationship between $A_{net}{}^{18}\Delta$ and cloud cover emerged. Indeed, in the low-LAI simulation, net photosynthetic isofluxes on DOY 198 reached higher peak values than on the partly cloudy days (DOY 196, 199, 204) that had the highest isofluxes in the base LAI case (Figure 10). This resulted from a combination of enhanced shade leaf photosynthesis and enriched $\delta^{18}O_{lw}$ due to a reduced transpiration feedback on canopy relative humidity. $\delta^{18}O_{lw}$ and $\delta^{18}O_c$ were even high enough on DOY 198 in the low-LAI simulation to briefly surpass the ~7.0‰ forest threshold (section 3.4.1), and $^{18}F_{la}$ reinforced $^{18}F_{al}$ to enrich $\delta^{18}O_a$ (Figure 10).

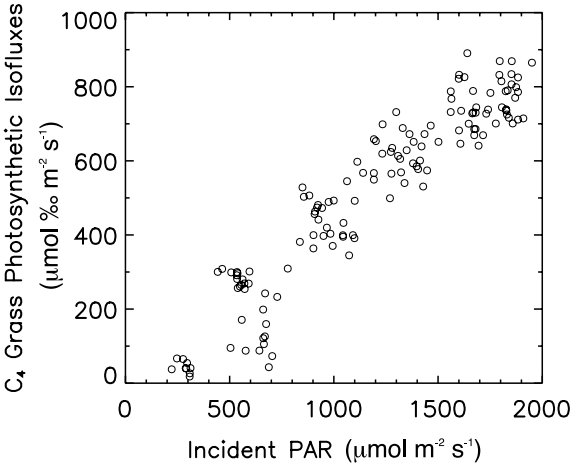

Figure 9. Modeled daytime net photosynthetic isofluxes ($A_{net}{}^{18}\Delta$, μmol ‰ m^{-2} s^{-1}) plotted against the observed daytime incident PAR for the C_4 grass canopy simulation.

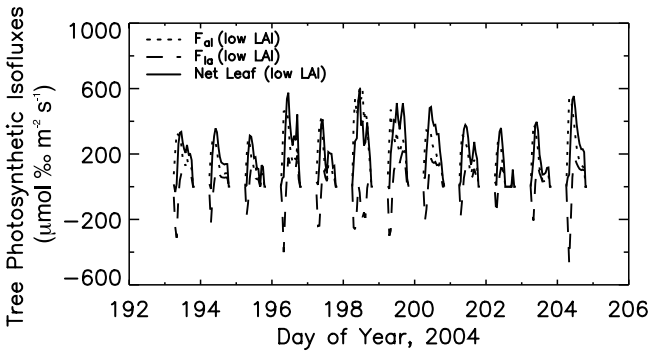

Figure 10. Modeled net photosynthetic isofluxes (μmol ‰ m^{-2} s^{-1}), $^{18}F_{al}$ and $^{18}F_{la}$, and their sum for the low-LAI (3.5) broadleaf tree canopy simulation.

3.5.2. C_4 Grassland

[52] We also assessed the sensitivity to LAI in the C_4 grass canopy, with other driving variables held constant. For these simulations, we decreased the LAI from the base case by one third (to a LAI of 2.5) and increased it twofold (to a LAI of 7.5). The reduced LAI lowered canopy photosynthesis and transpiration in the C_4 grassland relative to the base case. The expected response led to several changes that modified photosynthetic isofluxes, primarily via the same transpiration feedback on canopy relative humidity and $\delta^{18}O_{lw}$ that was found for the forest simulations. In particular, $\delta^{18}O_{lw}$ values increased in the reduced LAI simulations as the transpiration flux was lowered and the canopy relative humidity more closely tracked the observed, above-canopy humidity shown in Figure 2. Unlike the forest simulations, reducing LAI did not strengthen the relationship between leaf isofluxes and cloud cover. The negative response of C_4 photosynthesis to increasing cloud cover and R_D/R_S was similar for the different LAI values, and the isotope light response curve remained linear in all LAI simulations (Figure 9).

4. Discussion and Conclusions

[53] Terrestrial ecosystems are likely to respond to changes in irradiance, temperature, relative humidity, and R_D/R_S driven by changes in cloud cover. For example, *Min and Wang* [2008] showed that interannual cloud cover variations

drive interannual carbon fluxes in a temperate broadleaf forest. Clouds influence other ecological processes like shoot growth and reproduction [*Graham et al.*, 2003], photosynthesis of understory species [*Johnson and Smith*, 2006, 2008], tree growth [*Williams et al.*, 2008], and range boundaries [*Fischer et al.*, 2009]. At the leaf scale, diffuse light is used less efficiently for photosynthesis than direct light [*Brodersen et al.*, 2008], whereas at the canopy scale, the opposite response is observed. *Yakir and Israeli* [1995] documented how artificially reducing irradiance reduced growth but increased ^{13}C discrimination in an experimental plantation; this result is buttressed by work showing that increasing R_D/R_S in a multilayer canopy model increases Ci/Ca and ^{13}C discrimination [*Knohl and Baldocchi*, 2008].

[54] Our results illustrate the myriad impacts that clouds have on biosphere-atmosphere $CO^{18}O$ exchanges. We examined a sequence of midsummer days in which the light intercepted by the canopy varied from irradiance dominated by direct beam radiation (sunny) to days with high total irradiance but an increasing diffuse fraction (partly cloudy) to days in which almost all irradiance was diffuse (cloudy). This variation allowed a detailed examination of the mechanisms that drive ecosystem isotopic states and exchanges, and to explore how ecological properties influence the mechanisms and responses. Although this study only examined a portion of the growing season, we can hypothesize that, when integrated to a larger scale, clouds have a substantial impact on biosphere-atmosphere $CO^{18}O$ exchanges through their varied impacts on direct and diffuse radiation, leaf temperature, relative humidity, leaf water enrichment, and bidirectional leaf fluxes (F_{al} and F_{la}). These effects vary strongly with canopy structure, LAI, precipitation $\delta^{18}O$, and photosynthetic pathway.

[55] The forest canopy increased photosynthesis with increasing cloud cover and R_D/R_S, whereas the C_4 grass canopy exhibited a negative response to both increasing cloud cover and R_D/R_S. The LUE of the forest canopy was strongly related to R_D and leaf temperature, whereas the grass canopy LUE was relatively insensitive to environmental conditions. Compared to sunny conditions, the forest canopy exhibited larger photosynthetic isofluxes on partly cloudy days. The response of forest leaf isofluxes to cloud cover depends strongly on LAI, primarily via a feedback of transpiration on canopy relative humidity and $\delta^{18}O_{lw}$. Whereas the relationship between forest canopy photosynthesis and cloud cover (i.e., Figure 4b) became stronger with increasing LAI, the relationship between canopy photosynthetic isofluxes ($A_{net}{}^{18}\Delta$) and cloud cover weakened with increasing LAI.

[56] In contrast, photosynthesis and isofluxes in the C_4 grass canopy declined with increasing cloud cover and R_D/R_S, regardless of LAI. This opposite response resulted primarily from the lower effective shade leaf LAI in the lower-stature grass canopy compared to the broadleaf forest, as well as the near-constant light limitation on photosynthesis in C_4 sun and shade leaves. These different responses represent a fundamental functional distinction between these globally important vegetation types.

[57] It is important to acknowledge some of the modeling limitations in the work reported here. One deficiency is the lack of a separate energy balance and leaf temperature calculation for shade leaves. High LAI values are not uncommon in many forests, and the fraction of canopy photosynthesis attributable to shade leaves increases with LAI. An incorrect shade leaf temperature will impact canopy $CO^{18}O$ exchanges in several ways. First, $\delta^{18}O_{lw}$ is sensitive to leaf temperature because of its impact on the saturation vapor pressure inside leaves. Second, each 1°C increase in leaf temperature reduces the equilibrium liquid-vapor fractionation by ~0.07‰ for typical ambient temperatures [*Horita and Wesolowski*, 1994], and also reduces the equilibration fractionation between CO_2 and H_2O by −0.2‰ [*Brenninkmeier et al.*, 1983]. Leaf temperature also influences the leaf surface relative humidity and stomatal conductance, which in turn impacts C_i and bidirectional CO_2 fluxes across stomata. Finally, leaf temperature affects photosynthesis and respiration [*Collatz et al.*, 1991, 1992]. However, we tested the sensitivity of our results by varying shade leaf temperature and found the impact to be small (not shown).

[58] We also tested the impact of varying photosynthetic capacity (V_{max}) between sun and shade leaves. When we halved shade leaf V_{max} in the forest simulation, there was no change in shade leaf or total canopy photosynthesis, simply because shade leaf photosynthesis is always light limited. This prediction confirms the results of *Leuning et al.* [1995], who showed with a multilayer canopy model that total photosynthesis of shaded leaves is insensitive to the nitrogen distribution within a canopy. And, as shown by *de Pury and Farquhar* [1997], even with nitrogen and photosynthetic capacity distributed between sun and shade leaves as a function of optical depth in the canopy, the photosynthetic rate of shade leaves is always limited by light (i.e., by electron transport rate) and not by Rubisco.

[59] We contend that these model limitations have small impacts on our conclusions. One could test this assumption by conducting similar site-scale analyses with a one-dimensional, multilayer canopy models that also included turbulent transport and leaf nitrogen variations within the canopy [e.g., *Baldocchi and Bowling*, 2003; *Knohl and Baldocchi*, 2008]. However, for predictions of the impact of cloudiness on ecosystem-atmosphere $CO^{18}O$ exchanges at regional to global scales, a sun/shade model like ISOLSM that has already been integrated into global climate models [*Noone et al.*, 2004; Buenning et al., manuscript in preparation, 2009] is preferable for computational reasons.

[60] Although the differences in the response to cloudiness between C_3 and C_4 vegetation is largely due to differing F_{al} and F_{la} and photosynthetic rates, there are additional physiological and anatomical differences that would further impact $CO^{18}O$ exchanges that we did not consider. The differences between forest and grassland isofluxes would have been even larger if we had reduced the C_4 grass carbonic anhydrase activity [*Gillon and Yakir*, 2001]. For the work presented here we assumed complete equilibration between CO_2 and $\delta^{18}O_{lw}$ for both vegetation types, as we were interested primarily in ecosystem responses to changes in cloud cover as mediated by canopy structure and photosynthetic pathway. Also, we lacked field data on equilibration in this region, and recent studies suggest conflicting results for assigning appropriate values in modeling studies. *Gillon and Yakir* [2001] suggest a mean equilibration value of 0.4 for C_4 grasses; recent work with C_4 corn plants suggests values closer to C_3 plants [*Affek et al.*, 2005]. Laboratory measurements with both wild-type and transgenic individuals

of a C_4 dicot also suggest higher values from *in vitro* carbonic anhydrase assays [*Cousins et al.*, 2006]. Moreover, a recent phylogenetic analysis suggests that reduced carbonic anhydrase activity may not be simply a trait of grasses with the C_4 photosynthetic pathway, but may be more widespread among tropical grass lineages, including several widespread and productive C_3 grass species [*Edwards et al.*, 2007]. We also did not consider the large $\delta^{18}O_{lw}$ enrichment observed along leaf veins of C_4 grasses [*Helliker and Ehleringer*, 2000], which can affect leaf $CO^{18}O$ fluxes.

[61] This study demonstrates the complex responses of terrestrial ecosystems to changes in cloud cover, particularly with respect to oxygen isotope fluxes of CO_2. The broadleaf forest and C_4 grassland are predicted to have fundamentally different responses to changes in cloud cover. Our findings also identify a potentially important feedback of transpiration on canopy relative humidity, $\delta^{18}O_{cv}$, and $\delta^{18}O_{lw}$, and thus on leaf-to-atmosphere CO_2 isofluxes. We believe that some of the unexplained variation in $\delta^{18}O_a$ is driven by changes in clouds given the strong responses we show here and decadal-scale changes in cloud cover and aerosols observed in many locations.

[62] **Acknowledgments.** We gratefully acknowledge support from the NOAA Climate Program Office (grant NA03OAR4310059). Data were obtained from the Atmospheric Radiation Measurement program sponsored by the U.S. Department of Energy, Office of Science, Office of Biological and Environmental Research, Environmental Sciences Division. We also acknowledge meteorological data support provided by the Oklahoma and Kansas Mesonet program. The U.S. Network for Isotopes in Precipitation (http://www.uaa.alaska.edu/enri/usnip/index.cfm) contributed $\delta^{18}O$ data for our simulations and was supported in part by NSF Earth System History program (0080952). Comments from anonymous reviewers and the associate editor improved the manuscript.

References

Ackerman, T. P., and G. Stokes (2003), The Atmospheric Radiation Measurement program, *Phys. Today*, *56*, 38–45, doi:10.1063/1.1554135.

Affek, H. P., M. J. Krisch, and D. Yakir (2005), Effects of intraleaf variations in carbonic anhydrase activity and gas exchange on leaf $C^{18}OO$ isoflux in *Zea mays*, *New Phytol.*, *169*(2), 321–329, doi:10.1111/j.1469-8137.2005.01603.x.

Allison, G. B., C. J. Barnes, and M. W. Hughes (1983), The distribution of deuterium and ^{18}O in dry soils 2. Experimental, *J. Hydrol.*, *64*(1–4), 377–397, doi:10.1016/0022-1694(83)90078-1.

Alton, P. B., P. North, J. Kaduk, and S. Los (2005), Radiative transfer modeling of direct and diffuse sunlight in a Siberian pine forest, *J. Geophys. Res.*, *110*, D23209, doi:10.1029/2005JD006060.

Aranibar, J. N., et al. (2006), Combining meteorology, eddy fluxes, isotope measurements, and modeling to understand environmental controls of carbon isotope discrimination at the canopy scale, *Global Change Biol.*, *12*, 710–730, doi:10.1111/j.1365-2486.2006.01121.x.

Asner, G. P., et al. (2003), Global synthesis of leaf area index observations: Implications for ecological and remote sensing studies, *Global Ecol. Biogeogr.*, *12*(3), 191–205, doi:10.1046/j.1466-822X.2003.00026.x.

Baldocchi, D. D., and D. R. Bowling (2003), Modelling the discrimination of $^{13}CO_2$ above and within a temperate broad-leaved forest canopy on hourly to seasonal time scales, *Plant Cell Environ.*, *26*, 231–244, doi:10.1046/j.1365-3040.2003.00953.x.

Barbour, M. M., J. S. Roden, G. D. Farquhar, and J. R. Ehleringer (2004), Expressing leaf water and cellulose oxygen isotope ratios as enrichment above source water reveals evidence of a Peclet effect, *Oecologia*, *138*(3), 426–435, doi:10.1007/s00442-003-1449-3.

Barbour, M. M., et al. (2007), A new measurement technique reveals temporal variation in $\delta^{18}O$ of leaf-respired CO_2, *Plant Cell Environ.*, *30*, 456–468, doi:10.1111/j.1365-3040.2007.01633.x.

Beale, C. V., and S. P. Long (1995), Can perennial C_4 grasses attain high efficiencies of radiant energy conversion in cool climates?, *Plant Cell Environ.*, *18*, 641–650, doi:10.1111/j.1365-3040.1995.tb00565.x.

Betts, A. K., and J. H. Ball (1998), FIFE surface climate and site-average dataset 1987–89, *J. Atmos. Sci.*, *55*(7), 1091–1108, doi:10.1175/1520-0469(1998)055<1091:FSCASA>2.0.CO;2.

Bonan, G. B. (1994), Comparison of two land surface process models using prescribed forcings, *J. Geophys. Res.*, *99*, 25,803–25,818, doi:10.1029/94JD02188.

Bonan, G. (1996), A land surface model (LSM version 1.0) for ecological, hydrological, and atmospheric studies: Technical description and user's guide, *Tech. Note TN-417+STR*, Natl. Cent. for Atmos. Res., Boulder, Colo.

Bonan, G. B., K. J. Davis, D. Baldocchi, D. Fitzjarrald, and H. Neumann (1997), Comparison of the NCAR LSM1 land surface model with BOREAS aspen and jack pine tower fluxes, *J. Geophys. Res.*, *102*, 29,065–29,076, doi:10.1029/96JD03095.

Bowen, G. J., and B. Wilkinson (2002), Spatial distribution of $\delta^{18}O$ in meteoric precipitation, *Geology*, *30*(4), 315–318, doi:10.1130/0091-7613(2002)030<0315:SDOOIM>2.0.CO;2.

Brenninkmeier, C., K. Kraft, and W. Mook (1983), Oxygen isotope fractionation between CO_2 and H_2O, *Isot. Geosci.*, *1*, 181–190.

Brodersen, C. R., T. C. Vogelmann, W. E. Williams, and H. L. Gorton (2008), A new paradigm in leaf-level photosynthesis: Direct and diffuse lights are not equal, *Plant Cell Environ.*, *31*, 159–164.

Campbell, J. L., S. Burrows, S. T. Gower, and W. B. Cohen (1999), BigFoot: Characterizing land cover, LAI, and NPP at the landscape scale for EOS/MODIS validation. Field manual 2.1, *Publ. 4937*, Environ. Sci. Div., Oak Ridge Natl. Lab., Oak Ridge, Tenn.

Cappa, C. D., M. B. Hendricks, D. J. DePaolo, and R. C. Cohen (2003), Isotopic fractionation of water during evaporation, *J. Geophys. Res.*, *108*(D16), 4525, doi:10.1029/2003JD003597.

Cernusak, L. A., J. S. Pate, and G. D. Farquhar (2002), Diurnal variation in the stable isotope composition of water and dry matter in fruiting *Lupinus angustifolius* under field conditions, *Plant Cell Environ.*, *25*, 893–907, doi:10.1046/j.1365-3040.2002.00875.x.

Cernusak, L. A., G. D. Farquhar, S. C. Wong, and H. Stuart-Williams (2004), Measurement and interpretation of the oxygen isotope composition of carbon dioxide respired by leaves in the dark, *Plant Physiol.*, *136*, 3350–3363, doi:10.1104/pp.104.040758.

Cernusak, L. A., G. D. Farquhar, and J. S. Pate (2005), Environmental and physiological controls over oxygen and carbon isotope composition of Tasmanian blue gum, Eucalyptus globulus, *Tree Physiol.*, *25*, 129–146.

Chapin, F. S., III, P. A. Matson, and H. A. Mooney (2002), *Principles of Terrestrial Ecosystem Ecology*, 436 pp., Springer, New York.

Choudhury, B. J. (2001), Modeling radiation- and carbon-use efficiencies of maize, sorghum, and rice, *Agric. For. Meteorol.*, *106*, 317–330, doi:10.1016/S0168-1923(00)00217-3.

Ciais, P., P. P. Tans, M. Trolier, J. W. C. White, and R. J. Francey (1995), A large Northern Hemisphere terrestrial CO_2 sink indicated by the $^{13}C/^{12}C$ ratio of atmospheric CO_2, *Science*, *269*, 1098–1102, doi:10.1126/science.269.5227.1098.

Ciais, P., et al. (1997a), A three-dimensional synthesis study of $\delta^{18}O$ in atmospheric CO_2: 1. Surface fluxes, *J. Geophys. Res.*, *102*, 5857–5872, doi:10.1029/96JD02360.

Ciais, P., et al. (1997b), A three-dimensional synthesis study of $\delta^{18}O$ in atmospheric CO_2: 2. Simulations with the TM2 transport model, *J. Geophys. Res.*, *102*, 5873–5883, doi:10.1029/96JD02361.

Collatz, G. J., et al. (1991), Physiological and environmental regulation of stomatal conductance, photosynthesis and transpiration: A model that includes a laminar boundary layer, *Agric. For. Meteorol.*, *54*, 107–136, doi:10.1016/0168-1923(91)90002-8.

Collatz, G. J., et al. (1992), Coupled photosynthesis-stomatal conductance model for leaves of C_4 plants, *Aust. J. Plant Physiol.*, *19*, 519–538.

Collatz, G. J., J. A. Berry, and J. S. Clark (1998), Effects of climate and atmospheric CO_2 partial pressure on the global distribution of C_4 grasses: Present, past, and future, *Oecologia*, *114*(4), 441–454, doi:10.1007/s004420050468.

Cooley, H. S., W. J. Riley, M. S. Torn, and Y. He (2005), Impact of agricultural practice on regional climate in a coupled land surface mesoscale model, *J. Geophys. Res.*, *110*, D03113, doi:10.1029/2004JD005160.

Cousins, A. B., M. R. Badger, and S. von Caemmerer (2006), A transgenic approach to understanding the influence of carbonic anhydrase on $C^{18}OO$ discrimination during photosynthesis, *Plant Physiol.*, *142*, 662–672, doi:10.1104/pp.106.085167.

Craig, H., and L. Gordon (1965), Deuterium and oxygen-18 variations in the ocean and the marine atmosphere, paper presented at Stable Isotopes in Oceanographic Studies and Paleotemperatures, Cons. Naz. delle Ric. Lab. di Geol. Nucl., Spoleto, Italy.

Cuntz, M., P. Ciais, G. Hoffmann, and W. Knorr (2003a), A comprehensive global three-dimensional model of $\delta^{18}O$ in atmospheric CO_2: 1. Validation of surface processes, *J. Geophys. Res.*, *108*(D17), 4527, doi:10.1029/2002JD003153.

Cuntz, M., P. Ciais, G. Hoffmann, C. E. Allison, R. J. Francey, W. Knorr, P. P. Tans, J. W. C. White, and I. Levin (2003b), A comprehensive global three-dimensional model of $\delta^{18}O$ in atmospheric CO_2: 2. Mapping the

atmospheric signal, *J. Geophys. Res.*, *108*(D17), 4528, doi:10.1029/2002JD003154.
Dai, A., K. E. Trenberth, and T. R. Karl (1999), Effects of clouds, soil moisture, precipitation, and water vapor on diurnal temperature range, *J. Clim.*, *12*, 2451–2473, doi:10.1175/1520-0442(1999)012<2451:EOCSMP>2.0.CO;2.
de Pury, D. G. G., and G. D. Farquhar (1997), Simple scaling of photosynthesis from leaves to canopies, *Plant Cell Environ.*, *20*, 537–557, doi:10.1111/j.1365-3040.1997.00094.x.
Dickinson, R. (1983), Land surface processes and climate-surface albedos and energy balance, *Adv. Geophys.*, *25*, 305–353.
Dong, X., B. Xi, and P. Minnis (2006), Observational evidence of changes in water vapor, clouds, and radiation at the ARM SGP site, *Geophys. Res. Lett.*, *33*, L19818, doi:10.1029/2006GL027132.
Dongmann, G., H. W. Nürnberg, H. Förstel, and K. Wagener (1974), On the enrichment of $H_2{}^{18}O$ in the leaves of transpiring plants, *Radiat. Environ. Biophys.*, *11*, 41–52, doi:10.1007/BF01323099.
Edwards, E. J., C. J. Still, and M. J. Donoghue (2007), The relevance of phylogeny to studies of global change, *Trends Ecol. Evol.*, *22*(5), 243–249, doi:10.1016/j.tree.2007.02.002.
Ehleringer, J. R., T. E. Cerling, and B. R. Helliker (1997), C4 photosynthesis, atmospheric CO_2, and climate, *Oecologia*, *112*(3), 285–299, doi:10.1007/s004420050311.
Evans, J. R., and F. Loreto (2000), Acquisition and diffusion of CO_2 in higher plant leaves, in *Photosynthesis: Physiology and Metabolism*, edited by R. C. Leegood, T. D. Sharkey, and S. von Caemmerer, pp. 321–351, Kluwer Acad, Dordrecht, Netherlands.
Farquhar, G. D., and L. A. Cernusak (2005), On the isotopic composition of leaf water in the non-steady state, *Funct. Plant Biol.*, *32*(4), 293–303, doi:10.1071/FP04232.
Farquhar, G. D., and J. Lloyd (1993), Carbon and oxygen isotope effects in the exchange of carbon dioxide between plants and the atmosphere, in *Stable Isotopes and Plant Carbon-Water Relations*, edited by J. R. Ehleringer, A. E. Hall, and G. D. Farquhar, pp. 47–70, Academic, New York.
Farquhar, G. D., S. von Caemmerer, and J. A. Berry (1980), A biochemical model of photosynthetic CO_2 assimilation in leaves of C_3 species, *Planta*, *149*(1), 78–90, doi:10.1007/BF00386231.
Farquhar, G. D., J. R. Ehleringer, and K. T. Hubick (1989), Carbon isotope discrimination and photosynthesis, *Annu. Rev. Plant Physiol. Plant Mol. Biol.*, *40*, 503–537, doi:10.1146/annurev.pp.40.060189.002443.
Farquhar, G. D., et al. (1993), Vegetation effects on the isotope composition of oxygen in atmospheric CO_2, *Nature*, *363*, 439–443, doi:10.1038/363439a0.
Field, C. B., et al. (1998), Primary production of the biosphere: Integrating terrestrial and oceanic components, *Science*, *281*, 237–240, doi:10.1126/science.281.5374.237.
Fischer, D. T., C. J. Still, and A. P. Williams (2009), Significance of summer fog and overcast for drought stress and ecological functioning of coastal California endemic plant species, *J. Biogeogr.*, in press.
Flanagan, L. B. (2005), Ecosystem CO_2 exchange and variation in the $\delta^{18}O$ of atmospheric CO_2, in *Stable Isotopes and Biosphere-Atmosphere Interactions, Physiological Ecology*, edited by L. B. Flanagan, J. R. Ehleringer, and D. E. Pataki, pp. 171–181, Elsevier, San Diego, Calif.
Flanagan, L. B., et al. (1994), Effect of changes in leaf water oxygen isotopic composition on discrimination against $O^{18}O^{16}$ during photosynthetic gas exchange, *Aust. J. Plant Physiol.*, *21*, 221–234.
Förstel, H. (1978), The enrichment of ^{18}O in leaf water under natural conditions, *Radiat. Environ. Biophys.*, *15*, 323–344, doi:10.1007/BF01323459.
Francey, R. J., and P. P. Tans (1987), Latitudinal variation in oxygen-18 of atmospheric CO_2, *Nature*, *327*, 495–497, doi:10.1038/327495a0.
Freedman, J. M., D. R. Fitzjarrald, K. E. Moore, and R. K. Sakai (2001), Boundary layer clouds and vegetation-atmosphere feedbacks, *J. Clim.*, *14*, 180–197, doi:10.1175/1520-0442(2001)013<0180:BLCAVA>2.0.CO;2.
Friedli, H., U. Siegenthaler, D. Rauber, and H. Oeschger (1987), Measurements of concentration, $^{13}C/^{12}C$ and $^{18}O/^{16}O$ ratios of tropospheric carbon dioxide over Switzerland, *Tellus, Ser. B*, *39*, 80–88.
Fung, I., et al. (1997), Carbon 13 exchanges between the atmosphere and biosphere, *Global Biogeochem. Cycles*, *11*, 507–533, doi:10.1029/97GB01751.
Gillon, J. S., and D. Yakir (2000), Naturally low carbonic anhydrase activity in C_4 and C_3 plants limits discrimination against $C^{18}OO$ during photosynthesis, *Plant Cell Environ.*, *23*, 903–915, doi:10.1046/j.1365-3040.2000.00597.x.
Gillon, J., and D. Yakir (2001), Influence of carbonic anhydrase activity in terrestrial vegetation on the ^{18}O content of atmospheric CO_2, *Science*, *291*, 2584–2587, doi:10.1126/science.1056374.
Gower, S. T., C. J. Kucharik, and J. M. Norman (1999), Direct and indirect estimation of leaf area index, f_{APAR}, and net primary production of terrestrial ecosystems, *Remote Sens. Environ.*, *70*(1), 29–51, doi:10.1016/S0034-4257(99)00056-5.
Graham, E. A., S. S. Mulkey, K. Kitajima, N. G. Phillips, and S. J. Wright (2003), Cloud cover limits net CO_2 uptake and growth of a rainforest tree during tropical rainy seasons, *Proc. Natl. Acad. Sci. U. S. A.*, *100*, 572–576, doi:10.1073/pnas.0133045100.
Griffis, T. J., S. D. Sargent, J. M. Baker, X. Lee, B. D. Tanner, J. Greene, E. Swiatek, and K. Billmark (2008), Direct measurement of biosphere-atmosphere isotopic CO_2 exchange using the eddy covariance technique, *J. Geophys. Res.*, *113*, D08304, doi:10.1029/2007JD009297.
Gu, L., H. H. Shugart, J. D. Fuentes, T. A. Black, and S. R. Shewchuk (1999), Micrometeorology, biophysical exchanges and NEE decomposition in a two-story boreal forest—Development and test of an integrated model, *Agric. For. Meteorol.*, *94*, 123–148, doi:10.1016/S0168-1923(99)00006-4.
Gu, L., et al. (2001), Cloud modulation of surface solar irradiance at a pasture site in southern Brazil, *Agric. For. Meteorol.*, *106*, 117–129, doi:10.1016/S0168-1923(00)00209-4.
Gu, L., D. Baldocchi, S. B. Verma, T. A. Black, T. Vesala, E. M. Falge, and P. R. Dowty (2002), Advantages of diffuse radiation for terrestrial ecosystem productivity, *J. Geophys. Res.*, *107*(D6), 4050, doi:10.1029/2001JD001242.
Gu, L., et al. (2003), Response of a deciduous forest to the Mount Pinatubo eruption: Enhanced photosynthesis, *Science*, *299*, 2035–2038, doi:10.1126/science.1078366.
Harwood, K. G., J. S. Gillon, H. Griffiths, and M. S. J. Broadmeadow (1998), Diurnal variation in $\Delta^{13}CO_2$, $\Delta C^{18}O^{16}O$ and evaporative site enrichment of $\delta H_2{}^{18}O$ in *Piper aduncum* under field conditions in Trinidad, *Plant Cell Environ.*, *21*, 269–283, doi:10.1046/j.1365-3040.1998.00276.x.
Helliker, B. R., and J. R. Ehleringer (2000), Establishing a grassland signature in veins: ^{18}O in the leaf water of C_3 and C_4 grasses, *Proc. Natl. Acad. Sci. U. S. A.*, *97*, 7894–7898, doi:10.1073/pnas.97.14.7894.
Helliker, B. R., et al. (2002), A rapid and precise method for sampling and determining the oxygen isotope ratio of atmospheric water vapor, *Rapid Commun. Mass Spectrom.*, *16*, 929–932, doi:10.1002/rcm.659.
Hoag, K. J., C. J. Still, I. Y. Fung, and K. A. Boering (2005), Triple oxygen isotope composition of tropospheric carbon dioxide as a tracer of terrestrial gross carbon fluxes, *Geophys. Res. Lett.*, *32*, L02802, doi:10.1029/2004GL021011.
Hollinger, D. Y., et al. (1994), Carbon dioxide exchange between an undisturbed old-growth temperate forest and the atmosphere, *Ecology*, *75*(1), 134–150, doi:10.2307/1939390.
Hollinger, D. Y., et al. (1998), Forest-atmosphere carbon dioxide exchange in eastern Siberia, *Agric. For. Meteorol.*, *90*, 291–306, doi:10.1016/S0168-1923(98)00057-4.
Horita, J., and D. J. Wesolowski (1994), Liquid-vapor fractionation of oxygen and hydrogen isotopes of water from the freezing to the critical temperature, *Geochim. Cosmochim. Acta*, *58*(16), 3425–3437, doi:10.1016/0016-7037(94)90096-5.
Ishizawa, M., T. Nakazawa, and K. Higuchi (2002), A multi-box model study of the role of the biospheric metabolism in the recent decline of $\delta^{18}O$ in atmospheric CO_2, *Tellus, Ser. B*, *54*, 307–324.
Johnson, D. M., and W. K. Smith (2006), Low clouds and cloud immersion enhance photosynthesis in understory species of a southern Appalachian spruce-fir forest (USA), *Am. J. Bot.*, *93*(11), 1625–1632, doi:10.3732/ajb.93.11.1625.
Johnson, D. M., and W. K. Smith (2008), Cloud immersion alters microclimate, photosynthesis and water relations in *Rhododendron catawbiense* and *Abies fraseri* seedlings in the southern Appalachian Mountains, USA, *Tree Physiol.*, *28*, 385–392.
Jones, H. G. (1992), *Plants and Microclimate: A Quantitative Approach to Environmental Plant Physiology*, 428 pp., Cambridge Univ. Press, Cambridge, U.K.
Knohl, A., and D. D. Baldocchi (2008), Effects of diffuse radiation on canopy gas exchange processes in a forest ecosystem, *J. Geophys. Res.*, *113*, G02023, doi:10.1029/2007JG000663.
Lai, C.-T., J. R. Ehleringer, B. J. Bond, and U. K. T. Paw (2006a), Contributions of evaporation, isotopic non-steady state transpiration and atmospheric mixing on the $\delta^{18}O$ of water vapour in Pacific Northwest coniferous forests, *Plant Cell Environ.*, *29*, 77–94, doi:10.1111/j.1365-3040.2005.01402.x.
Lai, C.-T., W. Riley, C. Owensby, J. Ham, A. Schauer, and J. R. Ehleringer (2006b), Seasonal and interannual variations of carbon and oxygen isotopes of respired CO_2 in a tallgrass prairie: Measurements and modeling results from 3 years with contrasting water availability, *J. Geophys. Res.*, *111*, D08S06, doi:10.1029/2005JD006436.
Larcher, W. (2003), *Physiological Plant Ecology*, 4th ed., 513 pp., Springer, Berlin.
Lee, X., R. Smith, and J. Williams (2006), Water vapour $^{18}O/^{16}O$ isotope ratio in surface air in New England, USA, *Tellus, Ser. B*, *58*, 293–304.
Leuning, R., F. M. Kelliher, D. G. G. de Pury, and E.-D. Schulze (1995), Leaf nitrogen, photosynthesis, conductance and transpiration: Scaling

from leaves to canopy, *Plant Cell Environ.*, *18*, 1183–1200, doi:10.1111/j.1365-3040.1995.tb00628.x.
Liepert, B. G. (2002), rved reductions of surface solar radiation at sites in the United States and worldwide from 1961 to 1990, *Geophys. Res. Lett.*, *29*(10), 1421, doi:10.1029/2002GL014910.
Liepert, B. G., J. Feichter, U. Lohmann, and E. Roeckner (2004), Can aerosols spin down the water cycle in a warmer and moister world?, *Geophys. Res. Lett.*, *31*, L06207, doi:10.1029/2003GL019060.
Long, S. P. (1999), Environmental responses, in *C4 Plant Biology*, edited by R. F. Sage and R. K. Monson, pp. 215–249, Academic, New York.
Lynch, J. A., J. W. Grimm, and V. C. Bowersox (1995), Trends in precipitation chemistry in the United States: A national perspective, 1980–1992, *Atmos. Environ.*, *29*(11), 1231–1246, doi:10.1016/1352-2310(94)00371-Q.
McDowell, N., et al. (2008), Understanding the stable isotope composition of biosphere-atmosphere CO_2 exchange, *Eos Trans. AGU*, *89*(10), 94–95, doi:10.1029/2008EO100002.
Min, Q. (2005), Impacts of aerosols and clouds on forest-atmosphere carbon exchange, *J. Geophys. Res.*, *110*, D06203, doi:10.1029/2004JD004858.
Min, Q., and S. Wang (2008), Clouds modulate terrestrial carbon uptake in a midlatitude hardwood forest, *Geophys. Res. Lett.*, *35*, L02406, doi:10.1029/2007GL032398.
Morison, J. I. L., et al. (2000), Very high productivity of the C_4 aquatic grass *Echinochloa polystachya* in the Amazon floodplain confirmed by net ecosystem CO_2 flux measurements, *Oecologia*, *125*(3), 400–411, doi:10.1007/s004420000464.
Niyogi, D., et al. (2004), Direct observations of the effects of aerosol loading on net ecosystem CO_2 exchanges over different landscapes, *Geophys. Res. Lett.*, *31*, L20506, doi:10.1029/2004GL020915.
Noone, D., C. Still, W. Riley, L. Welp, and J. Randerson (2004), Isotopic diagnosis of processes governing interannual variability of $CO^{18}O$ fluxes in the tropics, *Eos Trans. AGU*, *85*(17), Jt. Assem. Suppl., Abstract B41B-02.
Norman, J. M., and T. J. Arkebauer (1991), Predicting canopy light-use efficiency from leaf characteristics, in *Modeling Plant and Soil Systems, Agronomy*, vol. 31, edited by J. Hanks and J. T. Ritchie, pp. 125–143, Am. Soc. of Agron., Madison, Wis.
Oliveira, P. H. F., et al. (2007), The effects of biomass burning aerosols and clouds on the CO_2 flux in Amazonia, *Tellus, Ser. B*, *59*, 338–349.
Ometto, J. P. H., L. B. Flanagan, L. A. Martinelli, and J. R. Ehleringer (2005), Oxygen isotope ratios of waters and respired CO_2 in Amazonian forest and pasture ecosystems, *Ecol. Appl.*, *15*(1), 58–70, doi:10.1890/03-5047.
Pearcy, R. W., and J. R. Ehleringer (1984), Comparative ecophysiology of C_3 and C_4 plants, *Plant Cell Environ.*, *7*, 1–13.
Peylin, P., et al. (1999), A 3-dimensional study of $\delta^{18}O$ in atmospheric CO_2: Contribution of different land ecosystems, *Tellus, Ser. B*, *51*, 642–667, doi:10.1034/j.1600-0889.1999.t01-2-00006.x.
Piedade, M. T. F., W. J. Junk, and S. P. Long (1991), The productivity of the C_4 grass *Echinochloa polystachya* on the Amazon floodplain, *Ecology*, *72*(4), 1456–1463, doi:10.2307/1941118.
Pinker, R. T., B. Zhang, and E. G. Dutton (2005), Do satellites detect trends in surface solar radiation?, *Science*, *308*, 850–854.
Price, D. T., and T. A. Black (1990), Effects of short-term variation in weather on diurnal canopy CO_2 flux and evapotranspiration of a juvenile Douglas-Fir stand, *Agric. For. Meteorol.*, *50*, 139–158.
Randerson, J. T., et al. (2002a), Carbon isotope discrimination of arctic and boreal biomes inferred from remote atmospheric measurements and a biosphere-atmosphere model, *Global Biogeochem. Cycles*, *16*(3), 1028, doi:10.1029/2001GB001435.
Randerson, J. T., G. J. Collatz, J. E. Fessenden, A. D. Munoz, C. J. Still, J. A. Berry, I. Y. Fung, N. Suits, and A. S. Denning (2002b), A possible global covariance between terrestrial gross primary production and ^{13}C discrimination: Consequences for the atmospheric ^{13}C budget and its response to ENSO, *Global Biogeochem. Cycles*, *16*(4), 1136, doi:10.1029/2001GB001845.
Rayner, P. J., I. G. Enting, R. J. Francey, and R. Langenfelds (1999), Reconstructing the recent carbon cycle from atmospheric CO_2, $\delta^{13}C$ and O_2/N_2 observations, *Tellus, Ser. B*, *51*, 213–232, doi:10.1034/j.1600-0889.1999.t01-1-00008.x.
Rayner, P. J., R. M. Law, C. E. Allison, R. J. Francey, C. M. Trudinger, and C. Pickett-Heaps (2008), Interannual variability of the global carbon cycle (1992–2005) inferred by inversion of atmospheric CO_2 and $\delta^{13}CO_2$ measurements, *Global Biogeochem. Cycles*, *22*, GB3008, doi:10.1029/2007GB003068.
Riley, W. J. (2005), A modeling study of the impact of the $\delta^{18}O$ value of near-surface soil water on the $\delta^{18}O$ value of the soil-surface CO_2 flux, *Geochim. Cosmochim. Acta*, *69*(8), 1939–1946, doi:10.1016/j.gca.2004.10.021.
Riley, W. J., C. J. Still, M. S. Torn, and J. A. Berry (2002), A mechanistic model of $H_2{}^{18}O$ and $C^{18}OO$ fluxes between ecosystems and the atmosphere: Model description and sensitivity analyses, *Global Biogeochem. Cycles*, *16*(4), 1095, doi:10.1029/2002GB001878.
Riley, W. J., et al. (2003), ^{18}O composition of CO_2 and H_2O ecosystem pools and fluxes in a tallgrass prairie: Simulations and comparisons to measurements, *Global Change Biol.*, *9*, 1567–1581, doi:10.1046/j.1365-2486.2003.00680.x.
Rocha, A. V., H.-B. Su, C. S. Vogel, H. P. Schmid, and P. S. Curtis (2004), Photosynthetic and water use efficiency responses to diffuse radiation by an aspen-dominated northern hardwood forest, *For. Sci.*, *50*(6), 793–801.
Roderick, M. L. (1999), Estimating the diffuse component from daily and monthly measurements of global radiation, *Agric. For. Meteorol.*, *95*, 169–185, doi:10.1016/S0168-1923(99)00028-3.
Roderick, M. L. (2006), The ever-flickering light, *Trends Ecol. Evol.*, *21*(1), 3–5, doi:10.1016/j.tree.2005.11.005.
Roderick, M. L., G. D. Farquhar, S. L. Berry, and I. R. Noble (2001), On the direct effect of clouds and atmospheric particles on the productivity and structure of vegetation, *Oecologia*, *129*(1), 21–30, doi:10.1007/s004420100760.
Sage, R. F., D. A. Wedin, and M. Li (1999), The biogeography of C_4 photosynthesis: Patterns and controlling factors, in *C4 Plant Biology*, edited by R. F. Sage and R. K. Monson, pp. 313–373, Academic, New York.
Scholze, M., J. O. Kaplan, W. Knorr, and M. Heimann (2003), Climate and interannual variability of the atmosphere-biosphere $^{13}CO_2$ flux, *Geophys. Res. Lett.*, *30*(2), 1097, doi:10.1029/2002GL015631.
Schwarz, A. G., and R. E. Redmann (1988), C_4 grasses from the boreal forest region of northwestern Canada, *Can. J. Bot.*, *66*, 2424–2430.
Seibt, U., L. Wingate, J. A. Berry, and J. Lloyd (2006), Non-steady state effects in diurnal ^{18}O discrimination by *Picea sitchensis* branches in the field, *Plant Cell Environ.*, *29*, 928–939, doi:10.1111/j.1365-3040.2005.01474.x.
Sellers, P. J. (1985), Canopy reflectance, photosynthesis and transpiration, *Int. J. Remote Sens.*, *6*, 1335–1372, doi:10.1080/01431168508948283.
Sellers, P. J., et al. (1996), A revised land surface parameterization (SiB2 for atmospheric GCMs. Part 1. Model formulation, *J. Clim.*, *9*, 676–705, doi:10.1175/1520-0442(1996)009<0676:ARLSPF>2.0.CO;2.
Stanhill, G., and S. Cohen (2001), Global dimming: A review of the evidence for a widespread and significant reduction in global radiation with discussion of its probable causes and possible agricultural consequences, *Agric. For. Meteorol.*, *107*, 255–278.
Stern, L. A., R. Amundson, and W. T. Baisden (2001), Influence of soils on oxygen isotope ratio of atmospheric CO_2, *Global Biogeochem. Cycles*, *15*, 753–759, doi:10.1029/2000GB001373.
Still, C. J., J. A. Berry, G. J. Collatz, and R. S. DeFries (2003), The global distribution of C_3 and C_4 vegetation: Carbon cycle implications, *Global Biogeochem. Cycles*, *17*(1), 1006, doi:10.1029/2001GB001807.
Still, C. J., et al. (2005), Simulation of ecosystem $C^{18}OO$ isotope fluxes in a tallgrass prairie: Biological and physical controls, in *Stable Isotopes and Biosphere-Atmosphere Interactions, Physiological Ecology*, edited by L. B. Flanagan, J. R. Ehleringer, and D. E. Pataki, pp. 154–170, Elsevier, San Diego, Calif.
Suyker, A. E., and S. B. Verma (2001), Year-round observations of the net ecosystem exchange of carbon dioxide in a native tallgrass prairie, *Global Change Biol.*, *7*, 279–289, doi:10.1046/j.1365-2486.2001.00407.x.
Turner, D. P., et al. (2003), A cross-biome comparison of daily light use efficiency for gross primary production, *Global Change Biol.*, *9*, 383–395, doi:10.1046/j.1365-2486.2003.00573.x.
Urban, O., et al. (2007), Ecophysiological controls over the net ecosystem exchange of mountain spruce stand: Comparison of the response in direct vs. diffuse solar radiation, *Global Change Biol.*, *13*, 157–168, doi:10.1111/j.1365-2486.2006.01265.x.
Vachon, R. W., J. W. White, E. Gutmann, and J. M. Welker (2007), Amount-weighted annual isotopic ($\delta^{18}O$) values are affected by the seasonality of precipitation: A sensitivity study, *Geophys. Res. Lett.*, *34*, L21707, doi:10.1029/2007GL030547.
von Caemmerer, S., and R. T. Furbank (2003), The C_4 pathway: An efficient CO_2 pump, *Photosynth. Res.*, *77*, 191–207, doi:10.1023/A:1025830019591.
Wang, X.-F., D. Yakir, and M. Avishai (1998), Non-climatic variations in the oxygen isotopic compositions of plants, *Global Change Biol.*, *4*, 835–849.
Wang, X. J., and J. R. Key (2003), Recent trends in arctic surface, cloud, and radiation properties from space, *Science*, *299*, 1725–1728, doi:10.1126/science.1078065.
Wang, Y.-P., and R. Leuning (1998), A two-leaf model for canopy conductance, photosynthesis and partitioning of available energy I: Model description and comparison with a multi-layered model, *Agric. For. Meteorol.*, *91*, 89–111, doi:10.1016/S0168-1923(98)00061-6.
Welker, J. (2000), Isotopic ($\delta^{18}O$) characteristics of weekly precipitation collected across the USA: An initial analysis with application to water source studies, *Hydrol. Processes*, *14*, 1449–1464, doi:10.1002/1099-1085(20000615)14:8<1449::AID-HYP993>3.0.CO;2-7.

Welp, L. R., J. T. Randerson, and H. P. Liu (2006), Seasonal exchange of CO_2 and $\delta^{18}O$-CO_2 varies with postfire succession in boreal forest ecosystems, *J. Geophys. Res.*, *111*, G03007, doi:10.1029/2005JG000126.

White, J. W. C., and S. D. Gedzelman (1984), The isotope composition of atmospheric water vapor and the concurrent meteorological conditions, *J. Geophys. Res.*, *89*, 4937–4939, doi:10.1029/JD089iD03p04937.

Wielicki, B. A., et al. (2002), Evidence for large decadal variability in the tropical mean radiative energy budget, *Science*, *295*, 841–844, doi:10.1126/science.1065837.

Wild, M., et al. (2005), From dimming to brightening: Decadal changes in surface solar radiation, *Science*, *308*, 847–850, doi:10.1126/science.1103215.

Wild, M., A. Ohmura, and K. Makowski (2007), Impact of global dimming and brightening on global warming, *Geophys. Res. Lett.*, *34*, L04702, doi:10.1029/2006GL028031.

Williams, A. P., C. J. Still, D. T. Fischer, and S. W. Leavitt (2008), The influence of summertime fog and overcast clouds on the growth of a coastal Californian pine: A tree-ring study, *Oecologia*, *156*(3), 601–611, doi:10.1007/s00442-008-1025-y.

Yakir, D., and Y. Israeli (1995), Reduced solar irradiance effects on net primary productivity (NPP) and the $\delta^{13}C$ and $\delta^{18}O$ values in plantations of *Musa* sp., *Musaceae*, *Geochim. Cosmochim. Acta*, *59*(10), 2149–2151, doi:10.1016/S0016-7037(99)80010-6.

Yakir, D., and L. D. L. Sternberg (2000), The use of stable isotopes to study ecosystem gas exchange, *Oecologia*, *123*(3), 297–311, doi:10.1007/s004420051016.

Zundel, G., W. Miekeley, B. M. Grisi, and H. Förstel (1978), The $H_2^{18}O$ enrichment in the leaf water of tropic trees: Comparison of species from the tropical rain forest and the semi-arid region in Brazil, *Radiat. Environ. Biophys.*, *15*, 203–212, doi:10.1007/BF01323265.

J. A. Berry, Department of Global Ecology, Carnegie Institution of Washington, Stanford, CA 94305, USA.

S. C. Biraud, W. J. Riley, and M. S. Torn, Earth Sciences Division, Lawrence Berkeley National Laboratory, Berkeley, CA 94720, USA.

N. H. Buenning and D. C. Noone, Department of Atmospheric and Oceanic Sciences, University of Colorado, Boulder, CO 80309, USA.

G. D. Farquhar, Research School of Biological Sciences, Australian National University, Canberra, ACT 0200, Australia.

J. T. Randerson, Earth System Science Department, University of California, Irvine, CA 92697, USA.

C. J. Still, Department of Geography, University of California, 3611 Elison Hall, Santa Barbara, CA 93106-4060, USA. (still@icess.ucsb.edu)

R. Vachon and J. W. C. White, INSTAAR, University of Colorado, Boulder, CO 80309, USA.

J. Welker, Environment and Natural Resources Institute, University of Alaska, Anchorage, AK 99508, USA.